Expanded Phylogenetic Diversity and Metabolic Flexibility of Microbial Mercury Methylation

Elizabeth A. McDaniel[1], Benjamin Peterson[1], Sarah L.R. Stevens[3,4], Patricia Q. Tran[1,2], Karthik Anantharaman[1], Katherine D. McMahon[1,5*]

[1] Department of Bacteriology, University of Wisconsin – Madison, Madison, WI

[2] Department of Integrative Biology, University of Wisconsin – Madison, Madison, WI

[3] Wisconsin Institute for Discovery, University of Wisconsin – Madison, Madison WI

[4] American Family Insurance Data Science Institute, University of Wisconsin – Madison, Madison WI

[5] Department of Civil and Environmental Engineering, University of Wisconsin – Madison, Madison WI

* Corresponding Author: kdmcmahon@wisc.edu

Running title: Diversity of microbial mercury methylation

ABSTRACT

Methylmercury is a potent, bioaccumulating neurotoxin that is produced by specific microorganisms by methylation of inorganic mercury released from anthropogenic sources. The *hgcAB* genes were recently discovered to be required for microbial methylmercury production in diverse anaerobic bacteria and archaea. However, the full phylogenetic and metabolic diversity of mercury methylating microorganisms has not been fully explored due to the limited number of cultured, experimentally verified methylators and the limitations of primer-based molecular methods. Here, we describe the phylogenetic diversity and metabolic flexibility of putative mercury methylating microorganisms identified by *hgcA* sequence identity from publicly available isolate genomes and metagenome-assembled genomes (MAGs), as well as novel freshwater MAGs. We demonstrate that putative mercury methylators are much more phylogenetically diverse than previously known, and the distribution of *hgcA* is most likely due to several independent horizontal gene transfer events. Identified methylating microorganisms possess diverse metabolic capabilities spanning carbon fixation, sulfate reduction, nitrogen fixation, and metal resistance pathways. Using a metatranscriptomic survey of a thawing permafrost gradient from which we identified 111 putative mercury methylators, we demonstrate that specific methylating populations may contribute to *hgcA* expression at different depths. Overall, we provide a framework for illuminating the microbial basis of mercury methylation using genome-resolved metagenomics and metatranscriptomics to identify methylators based upon *hgcA* presence and describe their putative functions in the environment.

IMPORTANCE

Specific anaerobic microorganisms among the *Deltaproteobacteria, Firmicutes*, and *Euryarchaeota* have been shown to produce the bioaccumulating neurotoxin methylmercury. Accurately assessing the sources of microbial methylmercury production in the context of phylogenetic identification, metabolic guilds, and activity in the environment is crucial for understanding the constraints and effects of mercury impacted sites. Advances in next-generation sequencing technologies have enabled large-scale, cultivation-independent surveys of diverse and poorly characterized microorganisms of numerous ecosystems. We used genome-resolved metagenomics and metatranscriptomics to highlight the vast phylogenetic and metabolic diversity of putative mercury methylators, and their depth-discrete activities in the environment. This work underscores the importance of using genome-resolved metagenomics to survey specific putative methylating populations of a given mercury-impacted ecosystem.

INTRODUCTION

Methylmercury is a potent neurotoxin that biomagnifies upward through food webs. Inorganic mercury deposited in sediments, freshwater, and the global ocean from both natural and anthropogenic sources is converted to the bioavailable and biomagnifying organic methylmercury (1, 2). Methylmercury production in the water column and sediments of freshwater lakes is one of the leading environmental sources that leads to fish consumption advisories (3, 4). Additionally, the majority of methylmercury exposure stems from contaminated marine seafood consumption (5). Consumption of methylmercury-contaminated fish is the most problematic for childbearing women and results in severe neuropsychological deficits when developed fetuses are exposed (6, 7). The biotransformation from inorganic to organic mercury is thought to be carried out by specific anaerobic microorganisms, namely sulfur-reducing (SRB) and iron-reducing (FeRB) bacteria and methanogenic archaea (8–10). Recently, the *hgcAB* genes were discovered to be required for mercury methylation. The *hgcA* gene encodes a corrinoid-dependent enzyme that is predicted to act as a methyltransferase, and *hgcB* encodes a 2[4Fe-4S] ferredoxin that reduces the corrinoid cofactor (11). Importantly, these genes are known to only occur in microorganisms capable of methylating mercury. This discovery has allowed for high-throughput identification of microorganisms with the potential to methylate mercury in diverse environmental datasets based upon *hgcAB* sequence presence (12, 13).

Currently, the known diversity of mercury methylating microorganisms has been described based on cultured isolates, amplicon sequencing of the 16S rRNA and/or *hgcA* loci of mercury impacted sites, *hgcA* quantitative PCR (qPCR) primers targeting specific

93 groups, or identification of *hgcA* on assembled metagenomic contigs (11, 13–20).
94 However, the complete phylogenetic and metabolic diversity of microorganisms capable
95 of methylating mercury is not fully understood due to previous efforts focusing on a few
96 cultured representatives, and poor predictive power of methylation potential based on
97 16S rRNA phylogenetic signal (8, 10, 21). Additionally, amplicon sequencing is limited in
98 detection of phylogenetic diversity, and the metabolic capabilities of these
99 microorganisms cannot be reliably studied using these techniques. Furthermore, a recent
100 study of microbial methylation in sulfate-impacted lakes demonstrated that 16S rRNA
101 amplicon-based surveys and *hgcA* clone libraries may not capture the true phylogenetic
102 diversity of many methylating microorganisms (22).

103 In this study, we identified nearly 1,000 genomes containing the *hgcA* marker from
104 publicly available isolate genomes, metagenome assembled genomes (MAGs), and
105 novel bins assembled from three freshwater lakes. Using this collection of MAGs and
106 reference genomes, we identified putative methylators spanning 30 phyla from diverse
107 ecosystems, some of which from phyla that, to our knowledge, have never been
108 characterized as methylating groups. The *hgcAB* phylogenetic signal suggests this
109 diverse region originated through extensive horizontal gene transfer events, and provides
110 insights into the difficulty of predicting methylation status using ribosomal sequences or
111 “universal” *hgcA* primers (17, 22). Putative methylators span metabolic guilds beyond
112 traditional sulfate and iron reducing bacteria and methanogenic archaea, carrying genes
113 for traits such as such as nitrogen fixation transformations and metal resistance
114 pathways. To understand *hgcA* expression in a potentially mercury impacted
115 environment, we analyzed depth-discrete metatranscriptomes from a permafrost thawing

gradient from which we identified 111 putative methylators. This work demonstrates the significance of reconstructing population genomes from mercury impacted environments to accurately capture the phylogenetic distribution and metabolic capabilities of key methylators in a given system.

MATERIALS AND METHODS

Accessed Datasets, Sampled Sites, and Metagenomic Assembly

We used a combination of publicly available MAGs, sequenced isolates, and newly assembled MAGs from three freshwater lakes. We sampled Lake Tanganyika in the East African Rift Valley, Lake Mendota in Madison, WI, and Trout Bog Lakes near Minocqua, WI. We collected depth-discrete samples along the northern basin of Lake Tanganyika at two stations (Kigoma and Mahale) (23). 24 samples were passed through a 0.2μm pore size-fraction filter, and used for shotgun metagenomic sequencing on the Illumina HiSeq 2500 platform at the Department of Energy Joint Genome Institute using previously reported methods with minor modifications (24). Each of the 24 metagenomes were individually assembled with MetaSPAdes and binned into population genomes using a combination of MetaBat, MetaBat2, and MaxBin. Across these binning approaches, approximately 4000 individual bins were assembled. To dereplicate identical bins assembled through different platforms, we applied DasTool (25) to keep the most representative bin for a given cluster, resulting in 803 total MAGs. Using a completeness/contamination cutoff of ≥70% and ≤10%, respectively, this resulted in approximately 431 MAGs. All dereplicated Lake Tanganyika genomes including identified

putative methylators are available through the JGI IMG portal under GOLD study ID Gs0129147.

Five depth-discrete samples were collected from the Lake Mendota hypolimnion using a peristaltic pump through acid-washed Teflon tubing onto a 0.2μm Whatman filter, and used for Illumina shotgun sequencing on the HiSeq4000 at the QB3 sequencing center in Berkeley, CA, USA. Samples were individually assembled using MetaSPAdes (26), and population genomes were constructed using a combination of the MetaBat2, Maxbin, and CONCOCT binning algorithms. Resulting MAGs were aggregated with DasTool and dereplicated into representative sets by pairwise average nucleotide identity comparisons (25). Population genomes from samples collected from Trout Bog Lake were assembled as previously described (24, 27, 28). All Trout Bog Lake MAGs including the 4 putative methylators are available through the JGI IMG portal under GOLD study ID Gs0063444. All publicly available isolate genomes and MAGs were accessed from Genbank in August of 2019, resulting in over 200,000 genomes in which to search for *hgcA.* Genomes from Jones et al. 2019 were accessed from JGI/IMG in March of 2019 at GOLD study ID Gs0130353 (22). Only genomes of medium quality according to MiMAG standards with > 50% completeness and < 10% redundancy were kept for downstream analyses, as calculated with CheckM (29, 30).

Identification of Putative Methylators

Using a collection of *hgcA* protein sequences from experimentally verified methylating organisms, we built a Hidden Markov Model (HMM) profile of the *hgcA* protein (11, 31). The constructed HMM profile was then used to identify putative mercury methylating bacteria and archaea. For all genome sequences, open reading frames and

protein-coding genes were predicted using Prodigal (32). Using the HMM profile built for the *hgcA* marker, we searched all protein sequences with an e-value cutoff of 1e-50. Sequence hits with an e-value cutoff score below 1e-50 and/or a score of 300 were removed from the results to ensure high confidence in all hits. All archaeal and bacterial *hgcA* hits were concatenated and aligned with MAFFT (33). Alignments were manually visualized using AliView (34), and sequences without the conserved cap-helix domain reported in Parks et al. 2013 were removed (11).

From this set of putative methylators, the taxonomy of each genome was assigned and/or confirmed using both an automatic and manual classification approach. Each genome was automatically classified using the genome taxonomy database toolkit (GTDB-tk) with default parameters (35). Additionally, each genome was manually classified using a set of 16 ribosomal protein markers (36). If a genome's taxonomy could not be resolved between the GTDB-tk classification and the manual ribosomal protein classification method, the genome was removed from the dataset (approximately 30 genomes). We kept specific genomes designated as "unclassified" as a handful of genomes with this designation belong to newly assigned phyla that have not been characterized in the literature, such as the proposed phyla BMS3A and Moduliflexota in the GTDB. This resulted in a total of 904 putative methylators used for downstream analyses as described. All genome information for each putative methylator including classification by each method, quality and genome statistics are provided in Supplementary Table 1 and summarized in Supplementary Figure 1.

hgcAB and Ribosomal Phylogenies

We selected the highest quality methylator from each phyla (total of 30 individual phyla containing a putative methylator) to place in a prokaryotic tree of life. Bacterial and archaeal references (the majority from Anantharaman et al. (37)) were screened for the 16 ribosomal protein HMMs along with the select 30 methylators. Individual ribosomal protein hits were aligned with MAFFT (33) and concatenated. The tree was constructed using FastTree and further visualized and edited using iTOL (38, 39) to highlight methylating phyla and novel methylating groups.

We created an HMM profile of *hgcB* from experimentally verified methylators as described above for *hgcA* (12, 40) From the set of 904 putative methylators identified by *hgcA* presence, we searched for *hgcB* by using a threshold cutoff score of 70 and requiring the resulting hit to either be directly downstream of *hgcA* or within five open reading frames, as some methylators have been observed to have genes between *hgcAB*. We recognize that this criterion might be overly conservative, potentially excluding some genomes with both genes (e.g. *hgcB* on a separate contig) but prefer to avoid any false positives. This resulted in 844 of 904 identified methylators also containing *hgcB*. To create a representative HgcAB tree to compare against a concatenated ribosomal protein phylogeny, a given genome had to contain 12 or more ribosomal protein markers to ensure accurate comparisons. Additionally, we removed sequences with low bootstrap support using RogueNaRok (41). Overall, this resulted in 650 HgcAB sequences to create a representative tree.

The HgcAB protein sequences were aligned separately using MAFFT and concatenated (33). The alignment was uploaded to the Galaxy server for filtering with BMGE1.1 using the BLOSUM30 matrix, a threshold and gap rate cutoff score of 0.5, and

206 a minimum block size of 5. (42, 43). A phylogenetic tree of the hits was constructed using
207 RaxML with 100 rapid bootstraps (44). The tree was automatically rooted and edited using
208 the interactive tree of life (iTOL) online tool (39). For visualization ease, we collapsed
209 clades by the dominant, monophyletic phyla when possible. For example, if a
210 monophyletic clade contained a majority (approximately 80-90%) of *Deltaproteobacteria*
211 sequences and one *Nitrospirae* sequence, we collapsed and identified the clade as a
212 whole as *Deltaproteobacteria*. This was done to broadly highlight the sparse phylogenetic
213 nature of identified HgcAB sequences. To reduce complexity, identified HgcAB
214 sequences of candidate phyla containing few individuals are not assigned individual
215 colors. The full phylogenetic tree with non-collapsed branches and most resolved
216 taxonomical names is provided in Supplementary Figure 2.

217 The corresponding ribosomal tree of the representative HgcAB sequences was
218 constructed using a collection of 16 ribosomal proteins provided in the metabolisHMM
219 package (36, 45). Each marker was searched for in each genome using specific HMM
220 profiles for each ribosomal protein, and individually aligned using MAFFT (33). Hits for
221 archaeal and bacterial taxa were concatenated separately to create an archaeal and
222 bacterial ribosomal protein tree. A phylogenetic tree was constructed with RAxML with
223 100 bootstraps and visualized using iTOL (44, 39).

224 **Functional Annotations, Metabolic Reconstructions, and *in silico* PCR analysis**

225 All genomes were functionally annotated using Prokka (46). Using the locus tag of
226 the predicted *hgcA* protein with the above HMM-based approach, the predicted gene
227 sequence for each *hgcA* open reading frame was obtained. *In silico* PCR of the universal
228 *hgcA* primers and group-specific qPCR *hgcA* primers were tested using Geneious

(Biomatters Ltd, Auckland, NZ), with primer sequences from Christensen et al. (20). The settings allows for both 0 and 2 mismatches, and the primer amplification "hit" results were compared to the full-genome classification of the given *hgcA* gene sequence. For genome synteny analysis of select permafrost methylators, Easyfig was used to generate pairwise BLAST results and view alignments (47). We did not use one of the *Myxococcales* MAGs as it was exactly identical to the other. The *Opitutae* genome GCA_003154355 from the UBA assembled set was not used because *hgcA* wsa found on only a very short contig.

Broad metabolic capabilities were characterized across all methylating organisms based on curated sets of metabolic HMM profiles provided in the metabolisHMM package (45, 37). An HMM of the putative transcriptional regulator was built using the alignment of the five putative transcriptional regulators with similar *hgcAB* sequences with muscle and hmmbuild (40, 48), and searched for among all methylators with hmmsearch (40). A genome was considered to have a hit for the putative transcriptional regulator if the identified protein contained a search hit e-value of greater than 1e-10 and was immediately upstream of *hgcAB* or 1-2 genes upstream. *Mer* genes for mercury transport were accessed from KofamKOALA using the corresponding threshold cutoff scores (49). Raw presence/absence results are provided in Supplementary Table 5.

Metabolic reconstruction of the MENDH-Thermoleophilia bin was supplemented with annotations using the KofamKOALA distribution of the KEGG database, and parsed for significant hits (49). The phylogeny of the MENDH-Thermoleophilia MAG was confirmed by downloading representative/reference sequences from Genbank and Refseq for the entire Actinobacteria phyla, depending on which database/designation was

252 available for the particular class. All Thermoleophilia class genomes were downloaded as
253 designated by the Genome Taxonomy Database (35). We included *Bacillus subtilis* strain
254 168 as an outgroup. The phylogeny was constructed using the alignment of concatenated
255 ribosomal proteins as described above. The tree was constructed using RAxML with 100
256 rapid bootstraps and visualized with iTOL (44, 39).

257 **Transcriptional Activity of Methylators in a Permafrost System**

258 To investigate the transcriptional activity of methylators in the environment, we
259 tracked activity of the identified methylating organisms in a permafrost thaw gradient
260 published by Woodcroft et al. 2018 (50). All 26 raw metatranscriptomes from the palsa,
261 bog, and fen sites were downloaded from NCBI. Adapters were removed and sequences
262 quality filtered with fastp (51). Each transcriptome was mapped to the indexed open
263 reading frames of the 111 putative methylators identified in this ecosystem using kallisto
264 (52). Annotated open reading frames and size in base pairs for each genome were
265 supplied using Prokka (46). For every sample, counts were normalized by calculating
266 transcripts per million (TPM), which equates for every 1 million reads in an RNA-seq
267 sample, “x” amount came from a certain gene/transcript. Briefly, TPM was calculated by
268 dividing the number of raw reads mapping to a given gene by dividing by the length of
269 that gene in base pairs. The sum of all normalized counts was divided by 1 million to
270 create a “per million” scaling factor. Each transcript’s normalized count is divided by the
271 1 million factor, which creates the final TPM value.

272 The *hgcA* open reading frame for each genome was identified by the
273 corresponding locus tag from the HMM profile annotation as described above. We did not
274 detect expression of any of the putative methylators in any of the palsa samples, and

therefore did not include these samples in the results. *hgcA* expression within a phylum was calculated by total TPM expression of *hgcA* within that phylum. Total *hgcA* expression within a sample was calculated as the total TPM-normalized expression of *hgcA* counts within that sample. The total average expression of methylators within a phylum was calculated by adding all TPM-normalized counts for all genomes within a phylum, and averaged by the number of genomes within that phyla to represent the average activity of that group compared to *hgcA* activity. Expression of *hgcA* was compared to the housekeeping gene *rpoB*, which encodes the RNA polymerase beta subunit. *rpoB* loci were predicted from Prokka annotations, and we compared expression between *hgcA* and *rpoB* at the phylum level. Normalized counts of *hgcA* and *rpoB* were summed within each phylum for each sample.

Data and Code Availability

Lake Tanganyika genomes have been deposited in Genbank under the project ID PRJNA523022 and are available at https://osf.io/pmhae/. The four Trout Bog genomes can be accessed from JGI/IMG under accession IDs 2582580680, 2582580684, 2582580694, and 2593339183. A complete workflow including all code and analysis workflows can be found at https://github.com/elizabethmcd/MEHG. All supplementary files including metadata, *hgcA* sequences and alignments, and tables are available on FigShare at https://figshare.com/account/home#/projects/70361 under the CC-BY 4.0 license.

RESULTS AND DISCUSSION

Identification of Diverse, Novel Putative Mercury Methylating Microorganisms

We identified nearly 1000 putative bacterial and archaeal mercury methylators spanning 30 phyla among publicly available isolate genomes and MAGs recovered from numerous environments (Figure 1). Well-known methylators among the *Deltaproteobacteria, Firmicutes, Euryarchaeota, and Bacteroidetes* represent well over half of all identified putative methylators, with the majority among the *Deltaproteobacteria* (Figure 1C). We also expanded upon groups of methylators that until recently have not been considered to be major contributors to mercury methylation. Putative methylators belonging to the *Spirochaetes* and the PVC superphylum (consisting of *Planctomycetes, Verrucomicrobia, Chlamydiae,* and *Lentisphaerae* phyla and several candidate divisions) have been identified from metagenomic contigs (13) and reconstructed MAGs from Jones et al (22). Additionally, *hgcA* sequences have been detected on metagenomic contigs belonging to the *Nitrospirae, Chloroflexi,* and *Elusimicrobia* (19, 53), but overall it is unknown how these groups contribute to methylmercury production. We identified putative methylators belonging to phyla that, to our knowledge, have not been previously described as mercury methylators. We identified 7 *Acidobacteria* methylators, 5 of which from the permafrost gradient system, in which these are considered to be the main plant biomass degraders (50). We also identified 17 *Actinobacterial* methylators, which all belong to poorly characterized lineages within the *Coriobacteria* and *Thermoleophilia* classes, as described below. A handful of putative methylators belong to recently described candidate phyla, such as Candidatus Aminicenantes, Candidatus Firestonebacteria, and WOR groups (Supplementary Figure 1D).

We reconstructed MAGs from three freshwater lakes with diverse biogeochemical characteristics. Lake Mendota is a large, dimictic, eutrophic lake in an urban setting in

Madison, WI, USA, with a sulfidic anoxic hypolimnion. Trout Bog Lake is a small, dimictic humic lake in a rural area near Minocqua, WI, that is surrounded by sphagnum moss, which leaches large amounts of organic carbon. Lake Tanganyika is a meromictic lake with an anoxic monimolimnion in the East African Rift Valley, and is the second largest lake in the world both by volume and depth, from which we recently reconstructed nearly 4000 MAGs from (23). From these reconstructed freshwater MAGs, we identified 55 putative mercury methylators. Several understudied *Verrucomicrobia* clades were recovered from the Lake Mendota hypolimnion. Members of this phylum are ubiquitous in freshwater and marine environments, display a cosmopolitan distribution, and can make up approximately 7% of the total microbial community in these ecosystems (28, 54–56). In Lake Mendota, members of the PVC superphylum account for approximately 40% of the microbial community in the hypolimnion, the majority of which do not contain *hgcA* (Peterson unpublished 2020).

A majority of the identified methylators were from subsurface aquifer system and thawing permafrost gradient assembled by Anantharaman et al. and Woodcroft et al., respectively (50, 57) (Figure 1B). Additionally, we identified methylators from hydrocarbon contaminated sites such as oil tills and sand ponds, sediments and wetlands, engineered systems, hydrothermal vents, and the built environment. A handful of methylating organisms were recovered from marine systems, as the Tara Ocean projects mostly includes samples from surface waters (58), and therefore would not include traditionally anaerobic methylating microorganisms. Interestingly, we identified marine endosymbionts of a mouthless, gutless worm (59), and Foraminifera spp. Although not as numerous as MAGs from various metagenomic surveys, we identified *hgcA* in over

150 isolate genomes, providing an expanded resource of isolates for experimentation (Supplementary Figure 1A). Using an extensive set of genomes mostly recovered from anoxic environments, we were able to greatly expand upon the known phylogenetic diversity of putative mercury methylating microorganisms.

Novel *Actinobacterial* Methylating Lineages

To our knowledge, members of the *Actinobacteria* have never been characterized as putative methylators or found to contain the *hgcA* marker. We identified 17 *Actinobacterial* putative methylators among diverse environments, including our Trout Bog and Lake Mendota freshwater datasets, as well as within the permafrost gradient and MAGs recovered from hydrocarbon contaminated sites (50, 60). In freshwater systems, *Actinobacteria* are ubiquitous and present a cosmopolitan distribution, with specific lineages comprising up to 50% of the total microbial community (61, 62). Freshwater *Actinobacteria* traditionally fall within the class *Actinobacteria*, but have a lower abundance distribution in the hypolimnion due to decreasing oxygen concentrations (63, 64). None of the *Actinobacterial* putative methylators belong to ubiquitous freshwater lineages.

All of the 17 identified *Actinobacterial* putative methylators belong to poorly described classes or ill-defined lineages that may branch outside of the established six classes of *Actinobacteria* (62). Nine fall within the *Coriobacteriia* class, four fall within the *Thermoleophilia* class, and the other four diverge from the existing *Actinobacteria* lineages. Three of the ill-defined *Actinobacterial* MAGs have been designated within the proposed class UBA1414, with two assembled from the permafrost system and one from the Lake Mendota hypolimnion. The other ill-defined *Actinobacterial* MAG was designated

367 within the proposed class RBG-13-55-18 and was also recovered from the permafrost
368 system. While some *Coriobacteriia* have been identified as clinically-significant members
369 of the human gut, all identified putative methylators belong to the OPB41 order (65), which
370 refers to the 16S rRNA sequence identified by Hugenholtz et al. from the Obsidian Pool
371 hot spring in Yellowstone National Park (66). Members of the OPB41 order have also
372 been found to subsist along the subseafloor of the Baltic Sea, an extreme and nutrient
373 poor environment (67).

374 Members of the *Thermoleophilia* are known as heat- and oil-loving microbes due
375 to their growth restriction to only substrate n-alkanes (68). Within this deep-branching
376 lineage, the two orders *Solirubrobacterales* and *Thermoleophilales* are currently
377 recognized based on sequenced isolates and the most updated version of Bergey's
378 Taxonomy (69, 70). However, our *Thermoleophilia* MAGs from the hypolimnia of Lake
379 Mendota and Trout Bog as well as two other putative *Thermoleophilia* methylators from
380 the permafrost thawing gradient do not cluster within the recognized orders (Figure 2).
381 According to the GTDB, these MAGs cluster within a novel order preliminarily named
382 UBA2241, as the only MAGs recovered from this novel order to-date have been from the
383 author's corresponding permafrost system (35, 50). Additionally, based on collected
384 isolates, members of the *Thermoleophilia* are assumed to be obligately aerobic (70).

385 The functional potential of *Thermoleophilia* members has been poorly described
386 due to few sequenced isolates and high-quality MAGs (71). We reconstructed the main
387 metabolic pathways of a high-quality *Thermoleophilia* MAG, referred to as MENDH-
388 Thermo (Supplementary Table 2). All components of the glycolytic pathway are present
389 for using a variety of carbohydrates for growth. A partial TCA cycle for providing reducing

power is present; only missing the step for converting citrate to isocitrate, which can be transported from outside sources. Interestingly, the MENDH-Thermo genome encodes the tetrahydromethanopterin-dependent *mch* and *fwdAB* enzymes, pointing to either formate utilization or detoxification (72, 73). We could not detect the presence of a putative acetate kinase, and therefore autotrophic growth through forming acetate is unlikely. Interestingly, the MENDH-Thermo genome encodes a full pathway for 4-Hydroxybutryate formation, a storage polymer (74). As the MENDH-Thermo genome can also synthesize the amino acids glycine and serine, combined with the ability to use reduced carbon compounds and form storage polymers, the MENDH-Thermo genome could exhibit a methylotrophic lifestyle, but is missing key steps for tetrahydromethanopterin cofactor synthesis and formate oxidation (75). The identification of putative methylators within the *Thermoleophilia* not only highlights novel metabolic features of putative methylators, but also of a poorly described class within the *Actinobacteria*.

Implications for Horizontal Gene Transfer of *hgcAB*

The HgcAB protein phylogeny exhibits patterns of extensive horizontal gene transfer (HGT) compared to a concatenated phylogeny of ribosomal proteins of corresponding genomes (Figure 3). For example, *Deltaproteobacterial* HgcAB sequences are some of the most disparate sequences surveyed, clustering with HgcAB sequences of *Actinobacteria, Nitrospirae, Spirochaetes,* and members of the PVC superphylum. Although *Firmicutes* HgcAB sequences are not as disparate, they also cluster with HgcAB sequences of other phyla such as *Deltaproteobacteria* and *Spirochaetes.* The only HgcAB sequences that cluster monophyletically among our dataset are the

413 *Bacteroidetes/Ignavibacteria* groups and *Nitrospirae*. These observations have
414 implications for the underlying evolutionary mechanisms of the methylation pathway and
415 modern methods for identifying methylating populations in the environment.

416 Gene gain/loss mediated through several HGT events have been previously
417 suggested to underpin the sparse and divergent phylogenetic distribution of *hgcAB* (11,
418 22). Metabolic functions can be horizontally transferred across diverse phyla through
419 numerous mechanisms, such as phage transduction, transposon-mediated insertion of
420 genomic islands or plasmid exchanges, direct conjugation, and/or gene gain/loss events.
421 We were unable to identify any *hgcA*-like sequences on any viral contigs in the NCBI
422 database or within close proximity to any known insertion sequences or transposases,
423 and all known *hgcA* sequences have been found on the chromosome. Structural and
424 mechanistic similarities between the cobalamin binding domains of HgcA and the carbon
425 monoxide dehydrogenase/acetyl-CoA synthase (CODH/ACS) of the reductive acetyl-CoA
426 pathway (also known as the Wood-Ljungdahl pathway) suggests associations between
427 the two pathways (11, 13). Interestingly, *hgcA* sequences of *Euryarchaeota* and
428 *Chloroflexi* cluster together, which was recently found to also be true for the CODH of
429 these groups (76). Inter-phylum HGT among anaerobic microorganisms has been
430 proposed to account for approximately 35% of metabolic genes and contributes to
431 functional redundancy across diverse phyla (77). It is plausible that a gene duplication
432 event followed by rampant gene gain/loss and independent transfers of both the CODH
433 and HgcA proteins could explain the disparate phylogeny, as has been respectively
434 described for both pathways (11, 13, 76).

435 To illustrate inter-phylum *hgcAB* HGT, we selected methylators assembled from a
436 permafrost system containing *hgcAB* regions with approximately 70% DNA sequence
437 similarity (Figure 4). Five methylators encompassing four different phyla (one
438 *Deltaproteobacteria,* two *Acidobacteria,* one *Verrucomicrobia,* and an *Actinobacteria)*
439 contain highly similar *hgcAB* regions, and the *hgcA* phylogeny does not match the
440 ribosomal protein phylogeny. All *hgcAB* sequences of these methylators are preceded by
441 a hypothetical protein that also shares sequence similarity among all methylators, but
442 which is annotated as a putative transcriptional regulator in the *Opitutae* genome. We
443 screened for this putative transcriptional regulator among all methylators in our dataset
444 and identified it immediately upstream of *hgcAB* in 112 genomes (Supplementary Table
445 3). Interestingly, we identified 12 genomes in which the putative transcriptional regulator
446 was upstream of *hgcAB*, but separated by one or two other genes. These genes were
447 mostly annotated as hypothetical proteins, but included esterases, oxidoreductases, and
448 methyltransferases. Otherwise, the gene neighborhoods of these similar permafrost
449 *hgcAB* sequences does not share any other obvious sequence or functional similarities.
450 The *hgcAB* genes are flanked by numerous hypothetical proteins, varying amino acid
451 synthesis and degradation genes, and oxidoreductases for core metabolic pathways.
452 Methylating populations have been identified in the environment through a
453 combination of nonspecific methods such as associations through 16S rRNA amplicon
454 sequencing (15, 78, 79), *hgcA* identification on metagenomic contigs (18, 53), universal
455 qPCR primers, and specific assays such as clade-specific qPCR primers (19, 20).
456 However, universal and clade-specific primers were constructed based on a handful of
457 experimentally verified methylators (20), which likely does not capture the complete or

458 true diversity of methylating microorganisms. We tested the accuracy of these primers *in*
459 *silico* on the coding regions of *hgcA* in all our identified putative methylators, using the
460 taxonomical assignment of each putative methylator from the full genome classification
461 (Supplementary Table 2). Depending on the number of *in silico* mismatches allowed, only
462 experimentally verified methylators could be identified, or *hgcA* sequences belonging to
463 other phyla would be hit (Supplementary Table 4). For example, *Deltaprobacterial*-
464 specific *hgcA* qPCR primers picked up related *Actinobacterial, Spirochaetes,* and
465 *Nitrospirae* sequences. Whereas the *Firmicutes*-specific primers did detect all
466 experimentally-verified *Firmicutes* methylators and a few environmental *hgcA* sequences,
467 overall they missed the diversity of *Firmicutes hgcA* sequences. Evidence of extensive
468 HGT of *hgcAB* across diverse phyla suggests that "universal" or even targeted guild
469 amplicon approaches may not be accurate. Instead, finer-scale primers of specific
470 methylating groups could be constructed based on recovered population genomes from
471 a specific environment containing *hgcAB* to ensure accuracy.

472 **Diversity of Metabolic Capabilities of Identified Methylators**

473 We next characterized the broad metabolic capabilities among high-quality
474 isolates and MAGs. From our analysis of metabolic profiles spanning several
475 biogeochemical cycles (37), *hgcA* is the only genetic marker linking high-quality
476 methylating genomes other than universally conserved markers (Figure 5). We detected
477 putative methylators with methanogenesis and sulfate reduction pathways, as is expected
478 for archaeal and bacterial methylating guilds, respectively (17, 22). Although the presence
479 of sulfate has been thought to select for methylating bacteria and drive methylation, very
480 few guilds we examined exhibited dissimilatory sulfate reduction pathways. We detected

481 machinery for dissimilatory sulfate reduction within the *Acidobacteria,*
482 *Deltaproteobacteria, Firmicutes,* and *Nitrospirae*. However, for example, only half of the
483 *Deltaproteobacterial* methylators screened contained the *dsrABD* subunits for sulfate
484 reduction. Similarly, we detected few guilds with the sulfate adenylyltransferase (*sat)*
485 marker for assimilatory sulfate reduction for incorporating sulfur into amino acids. This
486 suggests that mercury methylating groups may be composed of guilds other than
487 canonical SRBs and methanogenic archaea.

488 Interestingly, we found that several methylating guilds contain the essential
489 subunits that form the nitrogenase complex for nitrogen fixation. The three main
490 components of the nitrogenase complex are *nifH* and *nifD/nifK*, which encode the
491 essential iron and molybdenum-iron protein subunits, respectively. We detected
492 machinery for the nitrogenase complex within the *Acidobacteria, Actinobacteria,*
493 *Deltaproteobacteria, Euryarchaeota, Firmicutes, Nitrospirae,* and *Spirochaetes*
494 methylators. Notably, over half of all *Deltaproteobacterial* methylators and approximately
495 half of all *Firmicutes* methylators contain all three subunits for the nitrogenase complex.
496 Recently, the presence of nitrate has been suggested to regulate methylmercury
497 concentrations (80) leading to nitrate addition in an attempt to control methylmercury
498 accumulation in freshwater lakes (81). Although we detected parts of the denitrification
499 pathway in a handful of lineages, none of the putative methylators contained a full
500 denitrification pathway for fully reducing nitrate to nitrogen gas. Previous studies have
501 identified putative methylators among *Nitrospina* nitrite oxidizers in marine systems (18,
502 82). Although we did not detect putative *Nitrospina* methylators (possibly due to these

503 *hgcA* sequences being unbinned, within low-quality MAGs, or low-confidence hits), links
504 between the nitrogen cycle and mercury methylation warrants further exploration.

505 As mentioned above, structural and functional similarities between HgcA and the
506 carbon monoxide dehydrogenase/acetyl-CoA synthase (CODH/ACS) suggests
507 associations between the two pathways. This also raises the question if methylators use
508 the reductive acetyl-CoA pathway for autotrophic growth. We screened for the presence
509 of the codhC and codhD subunits of the carbon monoxide dehydrogenase, which have
510 been suggested as potential paralogous origins of HgcA (11, 13). Among high-quality
511 putative methylators, we detected both subunits among *Actinobacteria, Chloroflexi,*
512 *Deltaproteobacteria, Euryarchaeota, Firmicutes, Nitrospirae,* and members of the PVC
513 Superphylum. We also screened for the presence of the CODH catalytic subunit, which
514 would infer acetyl-CoA synthesis. Although we detected the CODH catalytic subunit, it
515 was not detected in all methylating lineages, such as the *Elusimicrobia, Synergistes,*
516 *Spirochaetes.* This suggests other growth strategies than autotrophic carbon fixation
517 among a large proportion of methylators, such as fermentation pathways as suggested
518 previously by Jones et al. (22).

519 Interestingly, over 50% of the putative methylators contain a thioredoxin dependent
520 arsenate reductase, which detoxifies arsenic through the reduction of arsenate to arsenite
521 (83, 84). As(V) reduction to the even more toxic As(III) is tightly coupled to export from
522 the cell, which has interesting similarities to the methylation system. Hg(II) uptake has
523 been shown to be energy dependent and therefore is imported through active transport
524 mechanisms (85). Hg(II) uptake is highly coupled to MeHg export, suggesting the
525 methylation system may act as a detoxification mechanism against environmental Hg(II)

526 (85). Interestingly, nearly none of the screened putative methylators contain the canonical
527 *mer* mercury resistance genes, including the *merA* mercury reductase to detoxify Hg(II)
528 to Hg(0). Additionally, very few members of the *Deltaproteobacteria, Euryarchaeota,* and
529 *Firmicutes* contain the *merP* periplasmic mercuric transporter, suggesting a different
530 mechanism for mercury transport and detoxification than the *mer* system. Overall,
531 putative methylators are composed of metabolic guilds other than the classical SRBs and
532 methanogenic archaea and employ diverse growth strategies other than autotrophic
533 carbon fixation.

534 **Expression of Putative Methylators in a Permafrost System**

535 While the connection between the presence of the *hgcA* marker and methylation
536 status has been well established in cultured isolates, there have been few studies
537 investigating *hgcA* transcriptional activity under laboratory conditions (86) or in a specific
538 environment (87). Additionally, the mere presence of a gene does not predict its functional
539 dynamics or activity in the environment. Assessing actively contributing microbial
540 populations to methylmercury production is important for identifying constraints on this
541 process. Genome-resolved metatranscriptomics provides an ideal approach for exploring
542 methylating population activity in the natural environment. Woodcroft et al. sampled
543 across three sites of the Stordalen Mire peatland in northern Sweden (50). This site
544 includes well-drained but mostly intact palsas, intermediately-thawed bogs with
545 *Sphagnum* moss, and completely thawed fens. Extensive spatiotemporal sampling paired
546 with genome-resolved metagenomic, metatranscriptomic, and metaproteomic
547 sequencing was applied to understand microbial contributions to carbon cycling along the
548 thawing gradient. We identified 111 putative methylators among MAGs assembled from

549 this permafrost system spanning well-known methylators belonging to the
550 *Deltaproteobacteria, Firmicutes*, and *Euryarchaeota*, but also less explored putative
551 methylators within the *Acidobacteria, Actinobacteria, Elusimicrobia*, and *Verrucomicrobia*.
552 We chose this extensive dataset to explore gene expression patterns of putative
553 methylators since it is largely an anaerobic environment, and has potential links for
554 methylmercury production due to the buildup of mercury gas beneath frozen permafrost
555 layers (88, 89).

556 We mapped the transcriptional reads for each sample to the open reading frames
557 of all identified putative methylators, normalized by transcripts per million (TPM). We
558 specifically investigated the depth-discrete expression patterns of *hgcA* within phylum-
559 level groups (Figure 6). We were unable to detect *hgcA* transcripts at any time-point or
560 depth among the palsa sites or the shallow bog depths, and therefore these sites and
561 depths are not included. The highest total *hgcA* transcript abundance was detected in the
562 fen sites, which is the most thawed along the permafrost gradient. The highest expression
563 of *hgcA* was contributed from the *Bacteroidetes* in the medium and deep depths of the
564 fen sites across multiple time-points, followed by those belonging to *Deltaproteobacteria*
565 in the medium and deep depths of the bog sites. Interestingly, *hgcA* expression in the bog
566 samples are almost exclusively dominated by *Deltaproteobacteria*, whereas the fen
567 samples contain a more diverse collection of phyla expressing *hgcA*, albeit *Bacteroidetes*
568 is the most dominant. Overall, methylators belonging to *Bacteroidetes* and
569 *Deltaproteobacteria* also constitute the most highly transcriptionally active members
570 across all samples.

All of the putative *Bacteroidetes* methylators transcribing *hgcA* belong to the vadinHA17 class. The name vadinHA17 was given to the 16S rRNA clone recovered from an anerobic digester treating winery wastewater, referring to the vinasses anerobic digestor of Narbonne (VADIN) (90). Members of the vadinHA17 group remain uncultured, and have been suggested to be involved in hydrolyzing and degrading complex organic matter, co-occurring with methanogenic archaea (91, 92). Currently, the three publicly available *Bacteroidetes* strains containing *hgcA* in belong to the *Paludibacteraceae* and *Marinilabiliaceae*, and are not closely related to members of the vadinHA17 class. However, the dominant *Deltaproteobacterial* member expressing *hgcA* in the bog samples is classified within the *Syntrophobacterales* order, specifically a member of *Smithella spp*. Among the publicly available sequenced Deltaproteobacterial isolates we identified *hgcA* in, 3 are among the *Syntrophobacterales* order, including the *Smithella* sp. F21 strain. This methylating strain may be an appealing experimental system to further explore *hgcA* expression patterns under different conditions.

We compared *hgcA* transcript abundance against that of the housekeeping gene *rpoB,* which encodes the RNA polymerase beta subunit, to differentiate *hgcA* activity against overall expression (Supplementary Figure 3). Low levels of *hgcA* expression were detected within the *Ignavibacteria, Chloroflexi, Euryarchaeota*, *Nitrospirae*, and *Planctomycetes*. Within the *Ignavibacteria* and *Chloroflexi*, expression of *rpoB* is on average higher in most samples than that of *hgcA.* This same trend occurs within the *Deltaproteobacteria*, where on average *rpoB* expression is higher than that of *hgcA*, although the majority of total *hgcA* transcripts within the bog sites is contributed to *Deltaproteobacterial* methylators. We did not detect *hgcA* transcripts within the

Aminicenantes and *Elusimicrobia*, but genomes within these groups exhibited low activity overall as shown by their *rpoB* expression. Interestingly, we found examples of genomes within phyla that exhibited appreciable amounts of overall transcriptional activity, but did not detect *hgcA* expression. We did not detect *hgcA* expression within the *Acidobacteria* or *Actinobacteria*, but did detect *rpoB* expression. These groups exhibited higher overall expression than groups in which we detected *hgcA* expression, such as the *Nitrospirae*.

This may have interesting implications for understanding methylmercury production in the environment, as currently the presence of *hgcAB* is used to connect specific microorganisms to biogeochemical characteristics. However, it may be possible that only a few groups exhibit *hgcA* activity and actually contribute to methylmercury production. Although this study does not contain environmental data on inorganic mercury or methylmercury concentrations, these results provide insights into *hgcA* expression for further follow-up.

CONCLUSIONS

In this study, we greatly expanded upon the known diversity of microorganisms that perform mercury methylation. We demonstrated using a set of publicly available isolate genomes, MAGs, and novel freshwater MAGs that putative methylators encompass 30 phylum-level lineages and diverse metabolic guilds. Apparent extensive HGT of the diverse *hgcAB* region poses unique challenges for screening methylating populations in the environment, in which “universal” amplicon or even group-specific approaches may not accurately reflect the true phylogenetic origin of specific methylators. Furthermore, genome-resolved metatranscriptomics of putative methylators in a thawing

permafrost system revealed that specific methylating populations are transcriptionally active at different sites and depths. These results highlight the importance of moving beyond identifying the mere presence of a gene to infer a specific function and investigating transcriptionally active populations. Overall, genome-resolved 'omics techniques are an appealing approach for accurately assessing the controls and constraints of microbial methylmercury production in the environment.

ACKNOWLEDGEMENTS

We would like to thank the many authors and groups for making a vast and valuable amount of genomic, metagenomic, and metatranscriptomic data publicly available, as our work was greatly improved by these datasets. We thank the U.S. National Science Foundation North Temperate Lakes Long-Term Ecological Research site (NTL-LTER DEB-1440297) for providing funding of the Microbial Observatory for long-term sampling of Lake Mendota and Trout Bog. Funding was also provided to KDM by the Wisconsin Alumni Research Foundation. We thank members of the McMahon lab for constructive feedback on drafts of the manuscript, specifically Amber White. We thank Kristopher Kieft and Adam Breister for providing NCBI viral searches and tree of life ribosomal sequences, respectively. We thank the U.S. Department of Energy Joint Genome Institute for sequencing and assembly (CSPs 394 and 2796). This research was performed in part using the computer resources and assistance of the Center for High-Throughput Computing (CHTC) at UW-Madison in the Department of Computer Sciences. CHTC is supported by UW-Madison, the Advanced Computing Initiative, the Wisconsin Alumni Research Foundation, the Wisconsin Institute for Discovery, and the

National Science Foundation. CHTC is an active member of the Open Science Grid, which is supported by the National Science Foundation and the U.S. Department of Energy Office of Science. Virtual machines were also accessed for computing through UW-Madison's Campus Computing Infrastructure. This research was also performed in part using the Wisconsin Energy Institute computing cluster, which is supported by the Great Lakes Bioenergy Research Center as part of the U.S. Department of Energy Office of Science.

REFERENCES

1. Wood JM. 1974. Biological cycles for toxic elements in the environment. Science 183:1049–52.
2. Chad R. Hammerschmidt* † and, Fitzgerald‡ WF. 2006. Methylmercury in Freshwater Fish Linked to Atmospheric Mercury Deposition.
3. Krabbenhoft DP. 2004. Methylmercury Contamination of Aquatic Ecosystems: A Widespread Problem with Many Challenges for the Chemical Sciences.
4. Hsu-Kim H, Kucharzyk KH, Zhang T, Deshusses MA. 2013. Mechanisms regulating mercury bioavailability for methylating microorganisms in the aquatic environment: A critical review. Environ Sci Technol 47:2441–2456.
5. Sunderland EM, Li M, Bullard K. 2018. Decadal Changes in the Edible Supply of Seafood and Methylmercury Exposure in the United States. Environ Health Perspect 126:17006.
6. Mahaffey KR, Clickner RP, Jeffries RA. 2009. Adult women's blood mercury concentrations vary regionally in the United States: Association with patterns of fish consumption (NHANES 1999-2004). Environ Health Perspect 117:47–53.
7. Schober SE, Sinks TH, Jones RL, Bolger PM, McDowell M, Osterloh J, Garrett ES, Canady RA, Dillon CF, Sun Y, Joseph CB, Mahaffey KR. 2003. Blood Mercury Levels in US Children and Women of Childbearing Age, 1999-2000. JAMA 289:1667.
8. Choi S-C, Chase T, Bartha R. 1994. Metabolic Pathways Leading to Mercury Methylation in Desulfovibrio desulfuricans LStAPPLIED AND ENVIRONMENTAL MICROBIOLOGY.

9. Kerin EJ, Gilmour CC, Roden E, Suzuki MT, Coates JD, Mason RP. 2006. Mercury Methylation by Dissimilatory Iron-Reducing Bacteria. Appl Environ Microbiol 72:7919–7921.

10. Yu R-Q, Reinfelder JR, Hines ME, Barkay T. 2013. Mercury methylation by the methanogen Methanospirillum hungatei. Appl Environ Microbiol 79:6325–30.

11. Parks JM, Johs A, Podar M, Bridou R, Hurt RA, Smith SD, Tomanicek SJ, Qian Y, Brown SD, Brandt CC, Palumbo A V, Smith JC, Wall JD, Elias DA, Liang L. 2013. The genetic basis for bacterial mercury methylation. Science 339:1332–5.

12. Gilmour CC, Podar M, Bullock AL, Graham AM, Brown SD, Somenahally AC, Johs A, Hurt RA, Bailey KL, Elias DA. 2013. Mercury methylation by novel microorganisms from new environments. Environ Sci Technol 47:11810–11820.

13. Podar M, Gilmour CC, Brandt CC, Soren A, Brown SD, Crable BR, Palumbo A V., Somenahally AC, Elias DA. 2015. Global prevalence and distribution of genes and microorganisms involved in mercury methylation. Sci Adv 1:e1500675–e1500675.

14. Bravo AG, Zopfi J, Buck M, Xu J, Bertilsson S, Schaefer JK, Poté J, Cosio C. 2018. Geobacteraceae are important members of mercury-methylating microbial communities of sediments impacted by waste water releases. ISME J 12:802–812.

15. Bravo AG, Peura S, Buck M, Ahmed O, Mateos-Rivera A, Ortega SH, Schaefer JK, Bouchet S, Tolu J, Björn E, Bertilsson S. 2018. Methanogens and iron-reducing bacteria: the overlooked members of mercury methylating microbial communities in boreal lakes. Appl Environ Microbiol AEM.01774-18.

16. Xu J, Buck M, Eklof K, Osman OA, Schaefer JK, Bishop K, Björn E, Skyllberg U, Bertilsson S, Bravo AG. 2018. Mercury methylating microbial communities of boreal forest soils. bioRxiv 299248.

17. Gilmour CC, Bullock AL, McBurney A, Podar M, Elias DA. 2018. Robust Mercury Methylation across Diverse Methanogenic Archaea. MBio 9:e02403-17.

18. Villar E, Cabrol L, Heimburger-Boavida LE. 2019. Widespread microbial mercury methylation genes in the global ocean. bioRxiv 648329.

19. Christensen GA, Gionfriddo CM, King AJ, Moberly JG, Miller CL, Somenahally AC, Callister SJ, Brewer H, Podar M, Brown SD, Palumbo A V., Brandt CC, Wymore AM, Brooks SC, Hwang C, Fields MW, Wall JD, Gilmour CC, Elias DA. 2019. Determining the Reliability of Measuring Mercury Cycling Gene Abundance with Correlations with Mercury and Methylmercury Concentrations. Environ Sci Technol 53:8649–8663.

20. Christensen GA, Wymore AM, King AJ, Podar M, Hurt RA, Santillan EU, Soren A, Brandt CC, Brown SD, Palumbo A V., Wall JD, Gilmour CC, Elias DA. 2016. Development and validation of broad-range qualitative and clade-specific quantitative molecular probes for assessing mercury methylation in the environment. Appl Environ Microbiol 82:6068–6078.

21. Ranchou-Peyruse M, Monperrus M, Bridou R, Duran R, Amouroux D, Salvado JC, Guyoneaud R. 2009. Overview of Mercury Methylation Capacities among Anaerobic Bacteria Including Representatives of the Sulphate-Reducers: Implications for Environmental Studies. Geomicrobiol J 26:1–8.

22. Jones DS, Walker GM, Johnson NW, Mitchell CPJ, Coleman Wasik JK, Bailey J

V. 2019. Molecular evidence for novel mercury methylating microorganisms in sulfate-impacted lakes. ISME J 1.

23. Tran PQ, McIntyre PB, Kraemer BM, Vadeboncoeur Y, Kimirei IA, Tamatamah R, McMahon KD, Anantharaman K. 2019. Depth-discrete eco-genomics of Lake Tanganyika reveals roles of diverse microbes, including candidate phyla, in tropical freshwater nutrient cycling. bioRxiv 834861.

24. Linz AM, He S, Stevens SLR, Anantharaman K, Rohwer RR, Malmstrom RR, Bertilsson S, McMahon KD. 2018. Freshwater carbon and nutrient cycles revealed through reconstructed population genomes. PeerJ 6:e6075.

25. Sieber CMK, Probst AJ, Sharrar A, Thomas BC, Hess M, Tringe SG, Banfield JF. 2018. Recovery of genomes from metagenomes via a dereplication, aggregation and scoring strategy. Nat Microbiol 1.

26. Nurk S, Meleshko D, Korobeynikov A, Pevzner PA. 2017. metaSPAdes: a new versatile metagenomic assembler. Genome Res 27:824–834.

27. Bendall ML, Stevens SL, Chan L-K, Malfatti S, Schwientek P, Tremblay J, Schackwitz W, Martin J, Pati A, Bushnell B, Froula J, Kang D, Tringe SG, Bertilsson S, Moran MA, Shade A, Newton RJ, McMahon KD, Malmstrom RR. 2016. Genome-wide selective sweeps and gene-specific sweeps in natural bacterial populations. ISME J 10:1589–1601.

28. He S, Stevens SLR, Chan L-K, Bertilsson S, Rio TG del, Tringe SG, Malmstrom RR, McMahon KD. 2017. Ecophysiology of Freshwater Verrucomicrobia Inferred from Metagenome-Assembled Genomes. mSphere 2:e00277-17.

29. Parks DH, Imelfort M, Skennerton CT, Hugenholtz P, Tyson GW. 2015. CheckM:

assessing the quality of microbial genomes recovered from isolates, single cells, and metagenomes. Genome Res 25:1043–55.

30. Bowers RM, Kyrpides NC, Stepanauskas R, Harmon-Smith M, Doud D, Reddy TBK, Schulz F, Jarett J, Rivers AR, Eloe-Fadrosh EA, Tringe SG, Ivanova NN, Copeland A, Clum A, Becraft ED, Malmstrom RR, Birren B, Podar M, Bork P, Weinstock GM, Garrity GM, Dodsworth JA, Yooseph S, Sutton G, Glöckner FO, Gilbert JA, Nelson WC, Hallam SJ, Jungbluth SP, Ettema TJG, Tighe S, Konstantinidis KT, Liu W-T, Baker BJ, Rattei T, Eisen JA, Hedlund B, McMahon KD, Fierer N, Knight R, Finn R, Cochrane G, Karsch-Mizrachi I, Tyson GW, Rinke C, Kyrpides NC, Schriml L, Garrity GM, Hugenholtz P, Sutton G, Yilmaz P, Meyer F, Glöckner FO, Gilbert JA, Knight R, Finn R, Cochrane G, Karsch-Mizrachi I, Lapidus A, Meyer F, Yilmaz P, Parks DH, Eren AM, Schriml L, Banfield JF, Hugenholtz P, Woyke T. 2017. Minimum information about a single amplified genome (MISAG) and a metagenome-assembled genome (MIMAG) of bacteria and archaea. Nat Biotechnol 35:725–731.

31. Eddy SR. 1996. Hidden Markov models. Curr Opin Struct Biol 6:361–365.

32. Hyatt D, Chen G-L, Locascio PF, Land ML, Larimer FW, Hauser LJ. 2010. Prodigal: prokaryotic gene recognition and translation initiation site identification. BMC Bioinformatics 11:119.

33. Katoh K, Misawa K, Kuma K, Miyata T. 2002. MAFFT: a novel method for rapid multiple sequence alignment based on fast Fourier transform. Nucleic Acids Res 30:3059–66.

34. Larsson A. 2014. AliView: a fast and lightweight alignment viewer and editor for

large datasets. Bioinformatics 30:3276–3278.

35. Parks DH, Chuvochina M, Waite DW, Rinke C, Skarshewski A, Chaumeil P-A, Hugenholtz P. 2018. A standardized bacterial taxonomy based on genome phylogeny substantially revises the tree of life. Nat Biotechnol 36:996.

36. Hug LA, Baker BJ, Anantharaman K, Brown CT, Probst AJ, Castelle CJ, Butterfield CN, Hernsdorf AW, Amano Y, Ise K, Suzuki Y, Dudek N, Relman DA, Finstad KM, Amundson R, Thomas BC, Banfield JF. 2016. A new view of the tree of life. Nat Microbiol 1:16048.

37. Anantharaman K, Brown CT, Hug LA, Sharon I, Castelle CJ, Probst AJ, Thomas BC, Singh A, Wilkins MJ, Karaoz U, Brodie EL, Williams KH, Hubbard SS, Banfield JF. 2016. Thousands of microbial genomes shed light on interconnected biogeochemical processes in an aquifer system. Nat Commun 7:13219.

38. Price MN, Dehal PS, Arkin AP. 2010. FastTree 2 – Approximately Maximum-Likelihood Trees for Large Alignments. PLoS One 5:e9490.

39. Letunic I, Bork P. 2016. Interactive tree of life (iTOL) v3: an online tool for the display and annotation of phylogenetic and other trees. Nucleic Acids Res 44:W242–W245.

40. Eddy SR. 2011. Accelerated Profile HMM Searches. PLoS Comput Biol 7:e1002195.

41. Aberer AJ, Krompass D, Stamatakis A. 2013. Pruning Rogue Taxa Improves Phylogenetic Accuracy: An Efficient Algorithm and Webservice. Syst Biol 62:162–166.

42. Afgan E, Baker D, Batut B, van den Beek M, Bouvier D, Čech M, Chilton J,

Clements D, Coraor N, Grüning BA, Guerler A, Hillman-Jackson J, Hiltemann S, Jalili V, Rasche H, Soranzo N, Goecks J, Taylor J, Nekrutenko A, Blankenberg D. 2018. The Galaxy platform for accessible, reproducible and collaborative biomedical analyses: 2018 update. Nucleic Acids Res 46:W537–W544.

43. Criscuolo A, Gribaldo S. 2010. BMGE (Block Mapping and Gathering with Entropy): a new software for selection of phylogenetic informative regions from multiple sequence alignments. BMC Evol Biol 10:210.

44. Stamatakis A. 2014. The RAxML v8 . 0 . X Manual 1–55.

45. McDaniel EA, Anantharaman K, McMahon KD. 2019. metabolisHMM: Phylogenomic analysis for exploration of microbial phylogenies and metabolic pathways. bioRxiv 2019.12.20.884627.

46. Seemann T. 2014. Prokka: rapid prokaryotic genome annotation. Bioinformatics 30:2068–2069.

47. Sullivan MJ, Petty NK, Beatson SA. 2011. Easyfig: A genome comparison visualizer. Bioinformatics 27:1009–1010.

48. Edgar RC. 2004. MUSCLE: multiple sequence alignment with high accuracy and high throughput. Nucleic Acids Res 32:1792–1797.

49. Aramaki T, Blanc-Mathieu R, Endo H, Ohkubo K, Kanehisa M, Goto S, Ogata H. 2019. KofamKOALA: KEGG ortholog assignment based on profile HMM and adaptive score threshold. bioRxiv 602110.

50. Woodcroft BJ, Singleton CM, Boyd JA, Evans PN, Emerson JB, Zayed AAF, Hoelzle RD, Lamberton TO, McCalley CK, Hodgkins SB, Wilson RM, Purvine SO, Nicora CD, Li C, Frolking S, Chanton JP, Crill PM, Saleska SR, Rich VI, Tyson

GW. 2018. Genome-centric view of carbon processing in thawing permafrost. Nature 560:49–54.

51. Chen S, Zhou Y, Chen Y, Gu J. 2018. fastp: an ultra-fast all-in-one FASTQ preprocessor. Bioinformatics 34:i884–i890.

52. Bray NL, Pimentel H, Melsted P, Pachter L. 2016. Near-optimal probabilistic RNA-seq quantification. Nat Biotechnol 34:525–527.

53. Podar M, Gilmour CC, Brandt CC, Soren A, Brown SD, Crable BR, Palumbo A V, Somenahally AC, Elias DA. 2015. Global prevalence and distribution of genes and microorganisms involved in mercury methylation. Sci Adv 1:1–13.

54. Tran P, Ramachandran A, Khawasik O, Beisner BE, Rautio M, Huot Y, Walsh DA. 2018. Microbial life under ice: Metagenome diversity and *in situ* activity of Verrucomicrobia in seasonally ice-covered Lakes. Environ Microbiol 20:2568–2584.

55. Chiang E, Schmidt ML, Berry MA, Biddanda BA, Burtner A, Johengen TH, Palladino D, Denef VJ. 2018. Verrucomicrobia are prevalent in north-temperate freshwater lakes and display class-level preferences between lake habitats. PLoS One 13:e0195112.

56. Cabello-Yeves PJ, Ghai R, Mehrshad M, Picazo A, Camacho A, Rodriguez-Valera F. 2017. Reconstruction of Diverse Verrucomicrobial Genomes from Metagenome Datasets of Freshwater Reservoirs. Front Microbiol 8:2131.

57. Anantharaman K, Brown CT, Hug LA, Sharon I, Castelle CJ, Probst AJ, Thomas BC, Singh A, Wilkins MJ, Karaoz U, Brodie EL, Williams KH, Hubbard SS, Banfield JF. 2016. Thousands of microbial genomes shed light on interconnected

biogeochemical processes in an aquifer system. Nat Commun 7:13219.

58. Tully BJ, Graham ED, Heidelberg JF. 2018. The reconstruction of 2,631 draft metagenome-assembled genomes from the global oceans. Sci Data 5:170203.

59. Woyke T, Teeling H, Ivanova NN, Huntemann M, Richter M, Gloeckner FO, Boffelli D, Anderson IJ, Barry KW, Shapiro HJ, Szeto E, Kyrpides NC, Mussmann M, Amann R, Bergin C, Ruehland C, Rubin EM, Dubilier N. 2006. Symbiosis insights through metagenomic analysis of a microbial consortium. Nature 443:950–955.

60. Parks DH, Rinke C, Chuvochina M, Chaumeil P-A, Woodcroft BJ, Evans PN, Hugenholtz P, Tyson GW. 2017. Recovery of nearly 8,000 metagenome-assembled genomes substantially expands the tree of life. Nat Microbiol 2:1533–1542.

61. Newton RJ, Jones SE, Eiler A, McMahon KD, Bertilsson S. 2011. A Guide to the Natural History of Freshwater Lake BacteriaMicrobiology and Molecular Biology Reviews.

62. Newton RJ, Jones SE, Helmus MR, McMahon KD. 2007. Phylogenetic Ecology of the Freshwater Actinobacteria acI Lineage. Appl Environ Microbiol 73:7169–7176.

63. Crump BC, Armbrust E V, Baross JA. 1999. Phylogenetic analysis of particle-attached and free-living bacterial communities in the Columbia river, its estuary, and the adjacent coastal ocean. Appl Environ Microbiol 65:3192–204.

64. Glöckner FO, Zaichikov E, Belkova N, Denissova L, Pernthaler J, Pernthaler A, Amann R. 2000. Comparative 16S rRNA analysis of lake bacterioplankton reveals globally distributed phylogenetic clusters including an abundant group of

actinobacteria. Appl Environ Microbiol 66:5053–65.

65. Bisanz JE, Soto-Perez P, Lam KN, Bess EN, Haiser HJ, Allen-Vercoe E, Rekdal VM, Balskus EP, Turnbaugh PJ. Illuminating the microbiome's dark matter: a functional genomic toolkit for the study of human gut Actinobacteria.

66. Hugenholtz P, Pitulle C, Hershberger KL, Pace NR. 1998. Novel division level bacterial diversity in a Yellowstone hot spring. J Bacteriol 180:366–76.

67. Bird JT, Tague ED, Zinke L, Schmidt JM, Steen AD, Reese B, Marshall IPG, Webster G, Weightman A, Castro HF, Campagna SR, Lloyd KG. 2019. Uncultured Microbial Phyla Suggest Mechanisms for Multi-Thousand-Year Subsistence in Baltic Sea Sediments. MBio 10:e02376-18.

68. Zarilla KA, Perry JJ. 1986. Deoxyribonucleic acid homology and other comparisons among obligately thermophilic hydrocarbonoclastic bacteria, with a proposal for Thermoleophilum minutum sp. nov. Int J Syst Bacteriol 36:13–16.

69. Ludwig W, Euzéby J, Schumann P, Busse H-J, Trujillo ME, Kämpfer P, Whitman WB. 2012. Road map of the phylum Actinobacteria, p. 1–28. *In* Bergey's Manual® of Systematic Bacteriology. Springer New York, New York, NY.

70. Suzuki K, Whitman WB. 2015. *Thermoleophilia class. nov.*, p. 1–4. *In* Bergey's Manual of Systematics of Archaea and Bacteria. John Wiley & Sons, Ltd, Chichester, UK.

71. Hu D, Zang Y, Mao Y, Gao B. 2019. Identification of Molecular Markers That Are Specific to the Class Thermoleophilia. Front Microbiol 10:1185.

72. Vorholt JA, Chistoserdova L, Stolyar SM, Thauer RK, Lidstrom ME. 1999. Distribution of tetrahydromethanopterin-dependent enzymes in methylotrophic

bacteria and phylogeny of methenyl tetrahydromethanopterin cyclohydrolases. J Bacteriol 181:5750–7.

73. Crowther GJ, Kosály G, Lidstrom ME. 2008. Formate as the main branch point for methylotrophic metabolism in Methylobacterium extorquens AM1. J Bacteriol 190:5057–5062.

74. Anderson AJ, Dawes EA. 1990. Occurrence, Metabolism, Metabolic Role, and Industrial Uses of Bacterial PolyhydroxyalkanoatesMICROBIOLOGICAL REVIEWS.

75. Chistoserdova L, Chen SW, Lapidus A, Lidstrom ME. 2003. Methylotrophy in Methylobacterium extorquens AM1 from a genomic point of view. J Bacteriol.

76. Adam PS, Borrel G, Gribaldo S. 2018. Evolutionary history of carbon monoxide dehydrogenase/acetyl-CoA synthase, one of the oldest enzymatic complexes. Proc Natl Acad Sci U S A 115:E1166–E1173.

77. Caro-Quintero A, Konstantinidis KT. 2015. Inter-phylum HGT has shaped the metabolism of many mesophilic and anaerobic bacteria. ISME J 9:958–967.

78. Xu J, Buck M, Eklöf K, Ahmed OO, Schaefer JK, Bishop K, Skyllberg U, Björn E, Bertilsson S, Bravo AG. 2019. Mercury methylating microbial communities of boreal forest soils. Sci Rep 9:518.

79. Vishnivetskaya TA, Hu H, Van Nostrand JD, Wymore AM, Xu X, Qiu G, Feng X, Zhou J, Brown SD, Brandt CC, Podar M, Gu B, Elias DA. 2018. Microbial community structure with trends in methylation gene diversity and abundance in mercury-contaminated rice paddy soils in Guizhou, China. Environ Sci Process Impacts 20:673–685.

916 80. Todorova SG, Driscoll CT, Matthews DA, Effler SW, Hines ME, Henry EA. 2009.
917 Evidence for Regulation of Monomethyl Mercury by Nitrate in a Seasonally
918 Stratified, Eutrophic Lake. Environ Sci Technol 43:6572–6578.
919 81. Matthews DA, Babcock DB, Nolan JG, Prestigiacomo AR, Effler SW, Driscoll CT,
920 Todorova SG, Kuhr KM. 2013. Whole-lake nitrate addition for control of
921 methylmercury in mercury-contaminated Onondaga Lake, NY. Environ Res
922 125:52–60.
923 82. Gionfriddo CM, Tate MT, Wick RR, Schultz MB, Zemla A, Thelen MP, Schofield
924 R, Krabbenhoft DP, Holt KE, Moreau JW. 2016. Microbial mercury methylation in
925 Antarctic sea ice. Nat Microbiol 1:16127.
926 83. Achour-Rokbani A, Cordi A, Poupin P, Bauda P, Billard P. 2010. Characterization
927 of the ars gene cluster from extremely arsenic-resistant Microbacterium sp. strain
928 A33. Appl Environ Microbiol 76:948–55.
929 84. Mukhopadhyay R, Rosen BP. 2002. Arsenate reductases in prokaryotes and
930 eukaryotes. Environ Health Perspect 110 Suppl 5:745–8.
931 85. Schaefer JK, Rocks SS, Zheng W, Liang L, Gu B, Morel FMM. 2011. Active
932 transport, substrate specificity, and methylation of Hg(II) in anaerobic bacteria.
933 Proc Natl Acad Sci U S A 108:8714–9.
934 86. Goñi-Urriza M, Corsellis Y, Lanceleur L, Tessier E, Gury J, Monperrus M,
935 Guyoneaud R. 2015. Relationships between bacterial energetic metabolism,
936 mercury methylation potential, and hgcA/hgcB gene expression in Desulfovibrio
937 dechloroacetivorans BerOc1. Environ Sci Pollut Res 22:13764–13771.
938 87. Bravo AG, Loizeau J-L, Dranguet P, Makri S, Björn E, Ungureanu VG,

939 Slaveykova VI, Cosio C. 2016. Persistent Hg contamination and occurrence of
940 Hg-methylating transcript (hgcA) downstream of a chlor-alkali plant in the Olt
941 River (Romania). Environ Sci Pollut Res 23:10529–10541.
942 88. Gordon J, Quinton W, Branfireun BA, Olefeldt D. 2016. Mercury and
943 methylmercury biogeochemistry in a thawing permafrost wetland complex,
944 Northwest Territories, Canada. Hydrol Process 30:3627–3638.
945 89. Schuster PF, Schaefer KM, Aiken GR, Antweiler RC, Dewild JF, Gryziec JD,
946 Gusmeroli A, Hugelius G, Jafarov E, Krabbenhoft DP, Liu L, Herman-Mercer N,
947 Mu C, Roth DA, Schaefer T, Striegl RG, Wickland KP, Zhang T. 2018. Permafrost
948 Stores a Globally Significant Amount of Mercury. Geophys Res Lett 45:1463–
949 1471.
950 90. Godon JJ, Zumstein E, Dabert P, Habouzit F, Moletta R. 1997. Molecular
951 microbial diversity of an anaerobic digestor as determined by small-subunit rDNA
952 sequence analysis. Appl Environ Microbiol 63:2802–2813.
953 91. Rojas P, Rodríguez N, de la Fuente V, Sánchez-Mata D, Amils R, Sanza JL.
954 2018. Microbial diversity associated with the anaerobic sediments of a soda lake
955 (Mono Lake, California, USA). Can J Microbiol 64:385–392.
956 92. Baldwin SA, Khoshnoodi M, Rezadehbashi M, Taupp M, Hallam S, Mattes A,
957 Sanei H. 2015. The microbial community of a passive biochemical reactor treating
958 arsenic, zinc, and sulfate-rich seepage. Front Bioeng Biotechnol 3.
959
960
961

962 **FIGURE LEGENDS**

963

964 **Figure 1. Phylogenetic Distribution and Diversity of Putative Methylators.**

965 Phylogenetic diversity and distribution of putative and novel methylators. **A)** Putative and
966 novel methylators among the prokaryotic tree of life. The highest quality methylator from
967 each identified phylum was selected as a representative among the tree of life. Purple
968 dots represent methylating phyla, and purple dots with stars represent phyla that, to our
969 knowledge, have not been identified as mercury methylators before this study. Groups in
970 bold and/or colored are methylating groups, whereas a few uncolored groups in non-bold
971 face are noted only for orientation. **B)** Number of putative methylating genomes found in
972 various environments, or genomes sequenced from isolates. **C)** Number of genomes
973 belonging to each phylum. Phylum names are given for all groups except the
974 *Deltaproteobacterial* class of *Proteobacteria*, as no putative *Proteobacterial* methylators
975 were identified outside of the *Deltaproteobacteria*. The group "other" contains several
976 candidate phyla and genomes within groups with few representatives, described in
977 Supplementary Figure 1.

978

979 **Figure 2. Novel Putative Methylators within the *Thermoleophilia* class of**
980 ***Actinobacteria***

981 Phylogenetic tree of publicly available and assembled *Thermoleophilia* MAGs and
982 *Actinobacteria* references. Representative or reference genomes belonging to the other
983 5 classes of *Actinobacteria* were used, with *Bacillus subtilis* used as an outgroup. Orders
984 are clustered and colored by GTDB proposed designation. The phylogeny was

985 constructed with RaxML using 100 rapid bootstraps, and nodes with bootstrap support
986 greater than 60 are shown as black circles. Stars denote putative methylators identified
987 in this study.
988
989 **Figure 3. Horizontal Gene Transfer of HgcAB Relative to Corresponding Ribosomal**
990 **Protein Phylogeny**
991 Phylogeny of HgcAB compared to a concatenated ribosomal protein phylogeny of select
992 methylators. **A)** Phylogeny of HgcAB of select methylators was constructed as described
993 in the Materials and Methods. The tree was constructed using RaxML with 100 rapid
994 bootstraps, and nodes with bootstrap support greater than 60 are depicted as a black
995 circle. **B)** Corresponding concatenated ribosomal protein phylogeny of the select
996 methylators. The tree was constructed using a set of 16 ribosomal proteins,
997 concatenated, and built using RaxML with 100 rapid bootstraps. Nodes with bootstrap
998 support of greater than 60 are denoted as a black circle. A fully annotated HgcAB tree is
999 provided in Supplementary Figure 2.
1000
1001 **Figure 4. Gene Neighborhoods of Diverse Permafrost Methylators Containing**
1002 **similar *hgcAB* Regions**
1003 Contigs containing similar *hgcAB* regions from putative methylators identified in a
1004 permafrost thawing system (50) were compared. Pairwise nucleotide BLAST between the
1005 genes for each contig was performed and visualized in easyfig (47). Colors correspond
1006 to predicted functions of each gene. *hgcAB* genes were identified based on curated

1007 HMMs and reference sequences, while all other gene assignments were made based on
1008 Prokka predictions.
1009
1010 **Figure 5. Metabolic Characteristics of Putative Methylators**
1011 Summary of broad metabolic characteristics present among high-quality putative
1012 methylators. Genomes with > 90% completeness and <10% redundancy and belonging
1013 to phyla with more than 5 genomes in that group were screened. HMM profiles spanning
1014 the sulfur, nitrogen, and carbon cycles, and metal resistance markers were searched for.
1015 The intensity of shading within a cell equates to the corresponding colored legend of
1016 percentage of genomes within that group that contain that marker. *hgcA* = Mercury
1017 methylation corrinoid protein, *arsC* = arsenite reductase, *codhCD/catalytic* = carbon
1018 monoxide dehydrogenase C,D, and catalytic subunits, *nifDHK* = nitrogenase subunits,
1019 *narGZ* = nitrate reductase subunits, *nirBDK* = nitrite reductase subunits, *norBD* = nitric
1020 oxide reductase subunits, *nosDZ* = nitrous oxide reductase subunits, *dsrABD* =
1021 dissimilatory sulfite reductase, *sat* = sulfate adenylyltransferase. Individual *nif, nar, nir,*
1022 *nor,* and *nos* subunit presence/absence results were averaged together, respectively.
1023
1024
1025 **Figure 6. Transcriptional Activity of Putative Methylators in a Permafrost Thawing**
1026 **Gradient**
1027 Mapped metatranscriptomic reads to 111 putative methylators identified in a permafrost
1028 thawing gradient (50). Bog and fen samples are shown, as no expression of *hgcA* was
1029 detected in any of the palsa samples. **Center)** Total reads mapping to the *hgcA* gene

within a phylum per sample normalized by transcripts per million (TPM). **Right)** Total *hgcA* counts per sample. **Top)** Average overall expression of genomes within a phylum across all samples.

Supplementary Figure 1. Overall Putative Methylating Genome and MAG Statistics **A)** Number of putative methylators that are isolates and the phylum they belong to. **B)** Estimated genome size of all putative methylators. **C)** Estimated GC content of all putative methylators **D)** Estimated genome size of putative methylating isolates. **E)** Estimated GC content of putative methylating isolates. **F)** Number of genomes belonging to "other" phyla designated in Figure 1B. **G)** Estimated genome size and GC content of various candidate phyla methylators. **H)** Estimated genome completeness and contamination of putative methylators that are MAGs. Only medium quality (>50% complete and <10% redundancy) putative methylating MAGs were included in the dataset.

Supplementary Figure 2. Full Annotated Reference HgcAB tree

Reference HgcAB tree of select methylators with uncollapsed nodes showing individual branch labels. Branch labels are sourced either from the name of the Genbank assembly, or custom name given to newly assembled Lake MAGs. Corresponding assembly names, classifications, and genome characteristics are provided in Supplementary Table 1. Available at https://figshare.com/account/projects/70361/articles/11620356

Supplementary Figure 3. Expression of *hgcA* compared to housekeeping gene *rpoB*

Comparison of expression of *hgcA* and the beta subunit of the RNA polymerase *rpoB* of putative methylators in the permafrost thawing gradient. Each data point is the sum of normalized counts by transcripts per million (TPM) within a sample for that phylum. Therefore all points of the boxplot are comparing total normalized counts of gene expression between different samples within a phylum. Expression of samples within palsa sites are not included since we did not detect any *hgcA* expression in any of these samples, and did not include these results in Figure 6.

SUPPLEMENTARY TABLES AND DATA FILES

All supplementary files are available at https://figshare.com/projects/Expanded_Diversity_and_Metabolic_Flexibility_of_Microbial_Mercury_Methylation/70361.

Supplementary Table 1. Genome Characteristics

Genome characteristics for all Genbank accessions and assembled freshwater MAGs containing confident *hgcA* hits. Available at https://figshare.com/articles/mehg-metadata/10062413

Supplementary Table 2. MENDH-Thermo Metabolic Reconstruction Annotations

Annotation results for specific pathways in the MENDH-Thermo MAG performed with Prokka and KofamKOALA. Available at https://figshare.com/account/projects/70361/articles/11620104

Supplementary Table 3. Putative Conserved *hgcAB* Regulator Results

Results for searching for putative conserved regulator of *hgcAB* found in permafrost methylators. Available at https://figshare.com/account/projects/70361/articles/11620107

Supplementary Table 4. Universal and Group-Specific *hgcA* Primer Results

In silco PCR results of universal and group-specific *hgcA* primer sets. The ORNL universal, Archaeal-specific, Deltaproteobacterial-specific, and Firmicutes-specific primer sets were ran in Genious allowing for both 0 and 2 mismatches, and matches with the taxonomical name in the metadata in Supplementary Table 1. Available at https://figshare.com/account/projects/70361/articles/10093535

Supplementary Table 5. Presence/Absence Matrix of Metabolic Markers Among High-Quality Methylators

Raw presence/absence matrix of select metabolic markers without the conversion of results greater than 1 converted to 1, due to uncertainty of copy number variation in MAGs. Available at https://figshare.com/account/projects/70361/articles/10203530

Data File 1. HgcA Hidden Markov Profile

Available at https://figshare.com/account/projects/70361/articles/10084610

Data File 2. FASTA Formatted file of all Identified HgcA Protein Sequences

Available at https://figshare.com/account/projects/70361/articles/10084601

Data File 3. HgcB Hidden Markov Profile

Available at https://figshare.com/account/projects/70361/articles/11620113

Data File 4: HgcAB Alignment

Available at https://figshare.com/account/projects/70361/articles/11620116

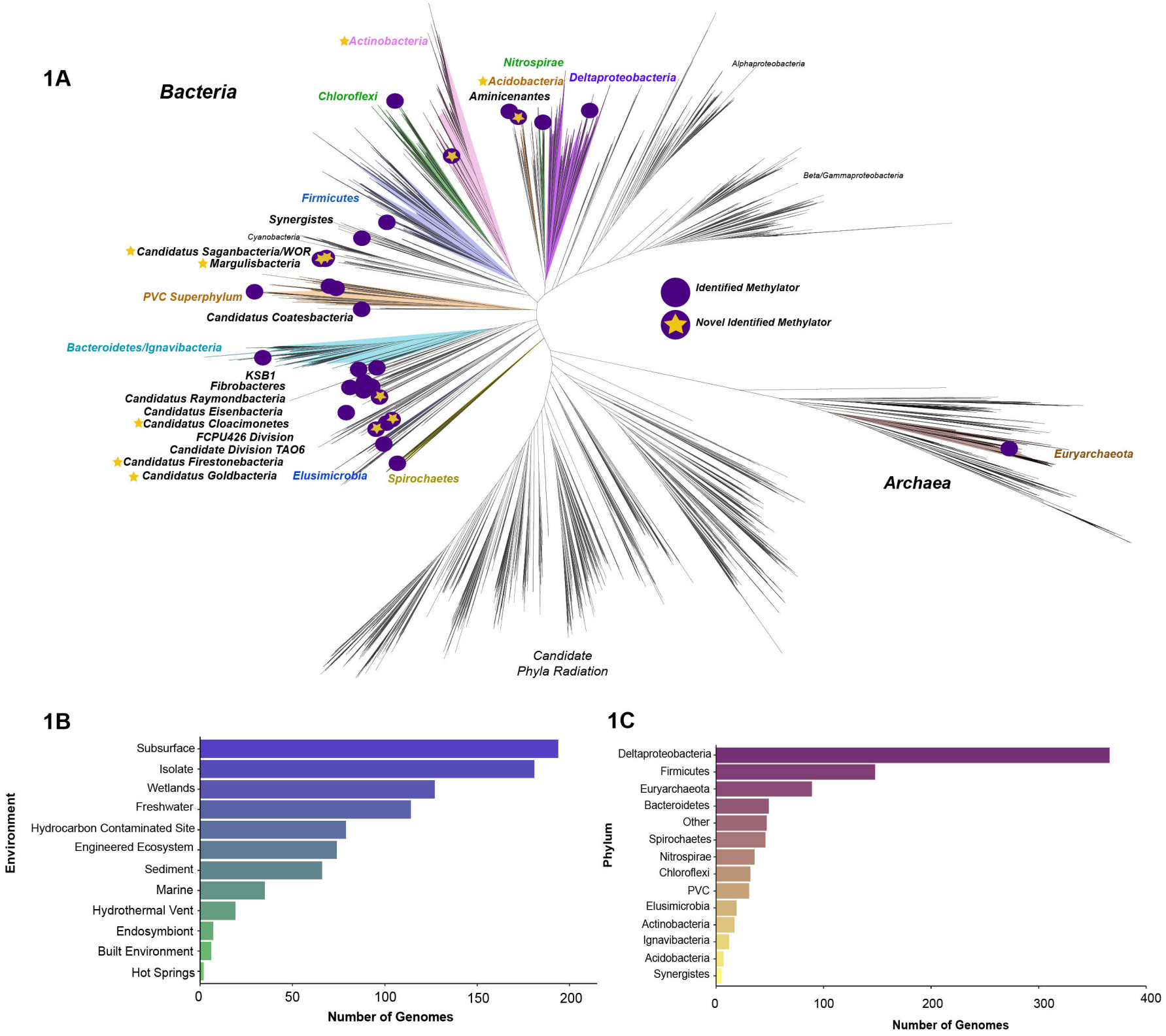
1A
Bacteria
Actinobacteria
Nitrospirae
Acidobacteria
Deltaproteobacteria
Aminicenantes
Alphaproteobacteria
Chloroflexi
Beta/Gammaproteobacteria
Firmicutes
Synergistes
Cyanobacteria
Candidatus Saganbacteria/WOR
Margulisbacteria
PVC Superphylum
Candidatus Coatesbacteria
Identified Methylator
Novel Identified Methylator
Bacteroidetes/Ignavibacteria
KSB1
Fibrobacteres
Candidatus Raymondbacteria
Candidatus Eisenbacteria
Candidatus Cloacimonetes
FCPU426 Division
Candidate Division TAO6
Candidatus Firestonebacteria
Candidatus Goldbacteria
Elusimicrobia
Spirochaetes
Euryarchaeota
Archaea
Candidate
Phyla Radiation
1B
Environment
Subsurface
Isolate
Wetlands
Freshwater
Hydrocarbon Contaminated Site
Engineered Ecosystem
Sediment
Marine
Hydrothermal Vent
Endosymbiont
Built Environment
Hot Springs
0
50
100
150
200
Number of Genomes
1C
Phylum
Deltaproteobacteria
Firmicutes
Euryarchaeota
Bacteroidetes
Other
Spirochaetes
Nitrospirae
Chloroflexi
PVC
Elusimicrobia
Actinobacteria
Ignavibacteria
Acidobacteria
Synergistes
0
100
200
300
400
Number of Genomes

2.

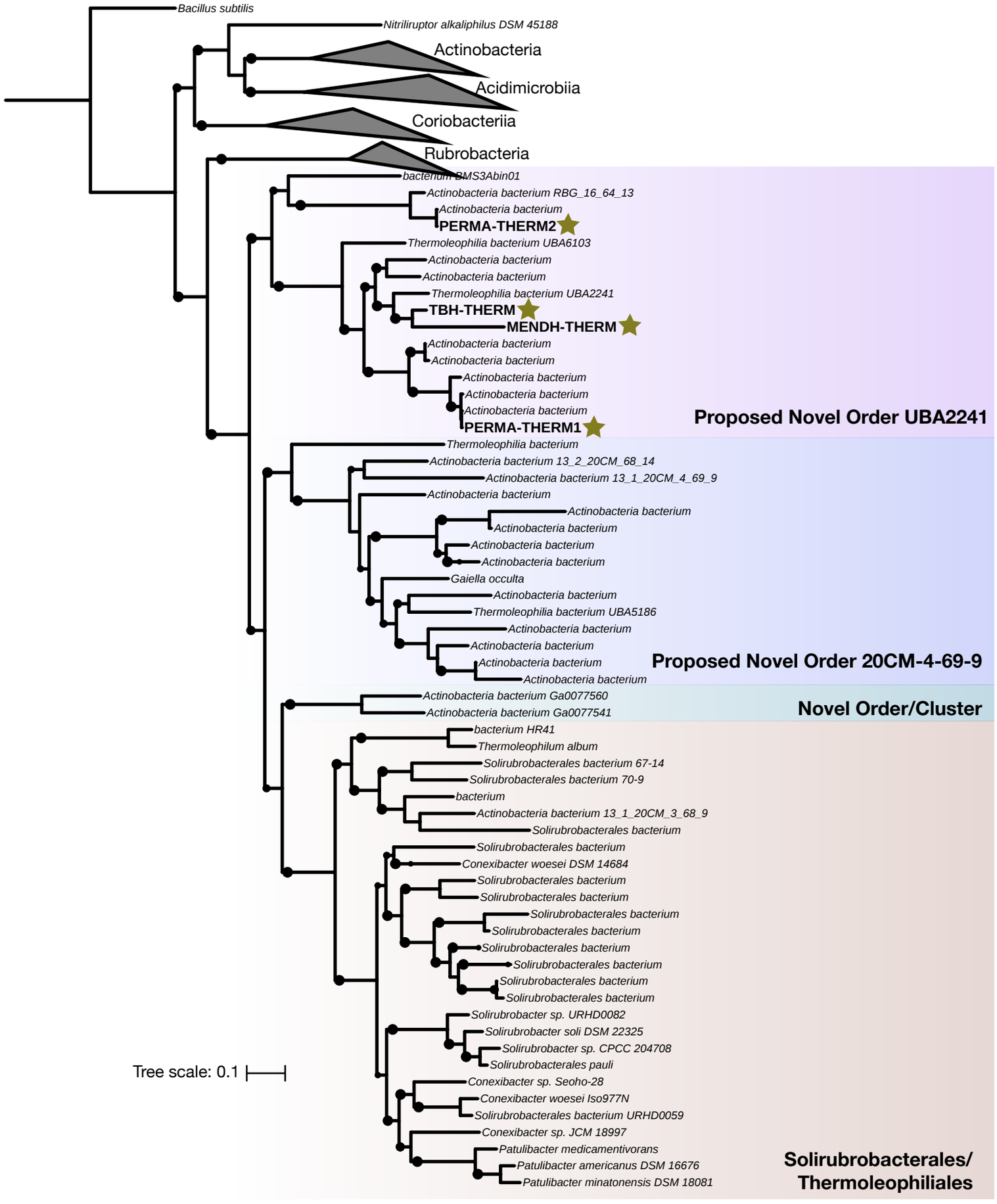

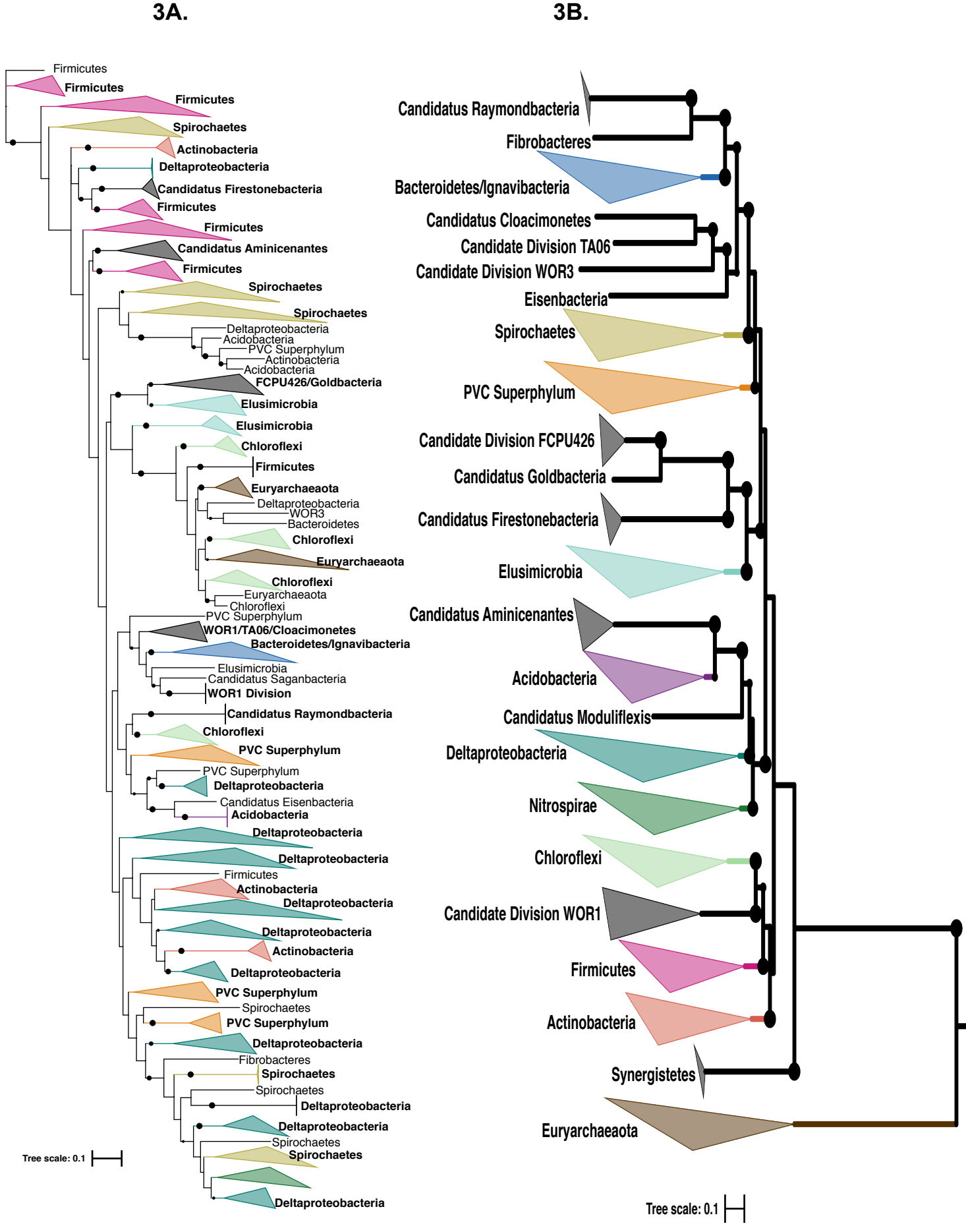
3A.
3B.
Firmicutes
Firmicutes
Firmicutes
Spirochaetes
Actinobacteria
Deltaproteobacteria
Candidatus Firestonebacteria
Firmicutes
Firmicutes
Candidatus Aminicenantes
Firmicutes
Spirochaetes
Spirochaetes
Deltaproteobacteria
Acidobacteria
PVC Superphylum
Actinobacteria
Acidobacteria
FCPU426/Goldbacteria
Elusimicrobia
Elusimicrobia
Chloroflexi
Firmicutes
Euryarchaeaota
Deltaproteobacteria
WOR3
Bacteroidetes
Chloroflexi
Euryarchaeaota
Chloroflexi
Euryarchaeaota
Chloroflexi
PVC Superphylum
WOR1/TA06/Cloacimonetes
Bacteroidetes/Ignavibacteria
Elusimicrobia
Candidatus Saganbacteria
WOR1 Division
Candidatus Raymondbacteria
Chloroflexi
PVC Superphylum
PVC Superphylum
Deltaproteobacteria
Candidatus Eisenbacteria
Acidobacteria
Deltaproteobacteria
Deltaproteobacteria
Firmicutes
Actinobacteria
Deltaproteobacteria
Deltaproteobacteria
Actinobacteria
Deltaproteobacteria
PVC Superphylum
Spirochaetes
PVC Superphylum
Deltaproteobacteria
Fibrobacteres
Spirochaetes
Spirochaetes
Deltaproteobacteria
Deltaproteobacteria
Spirochaetes
Spirochaetes
Deltaproteobacteria
Tree scale: 0.1
Candidatus Raymondbacteria
Fibrobacteres
Bacteroidetes/Ignavibacteria
Candidatus Cloacimonetes
Candidate Division TA06
Candidate Division WOR3
Eisenbacteria
Spirochaetes
PVC Superphylum
Candidate Division FCPU426
Candidatus Goldbacteria
Candidatus Firestonebacteria
Elusimicrobia
Candidatus Aminicenantes
Acidobacteria
Candidatus Moduliflexis
Deltaproteobacteria
Nitrospirae
Chloroflexi
Candidate Division WOR1
Firmicutes
Actinobacteria
Synergistetes
Euryarchaeaota
Tree scale: 0.1

4.

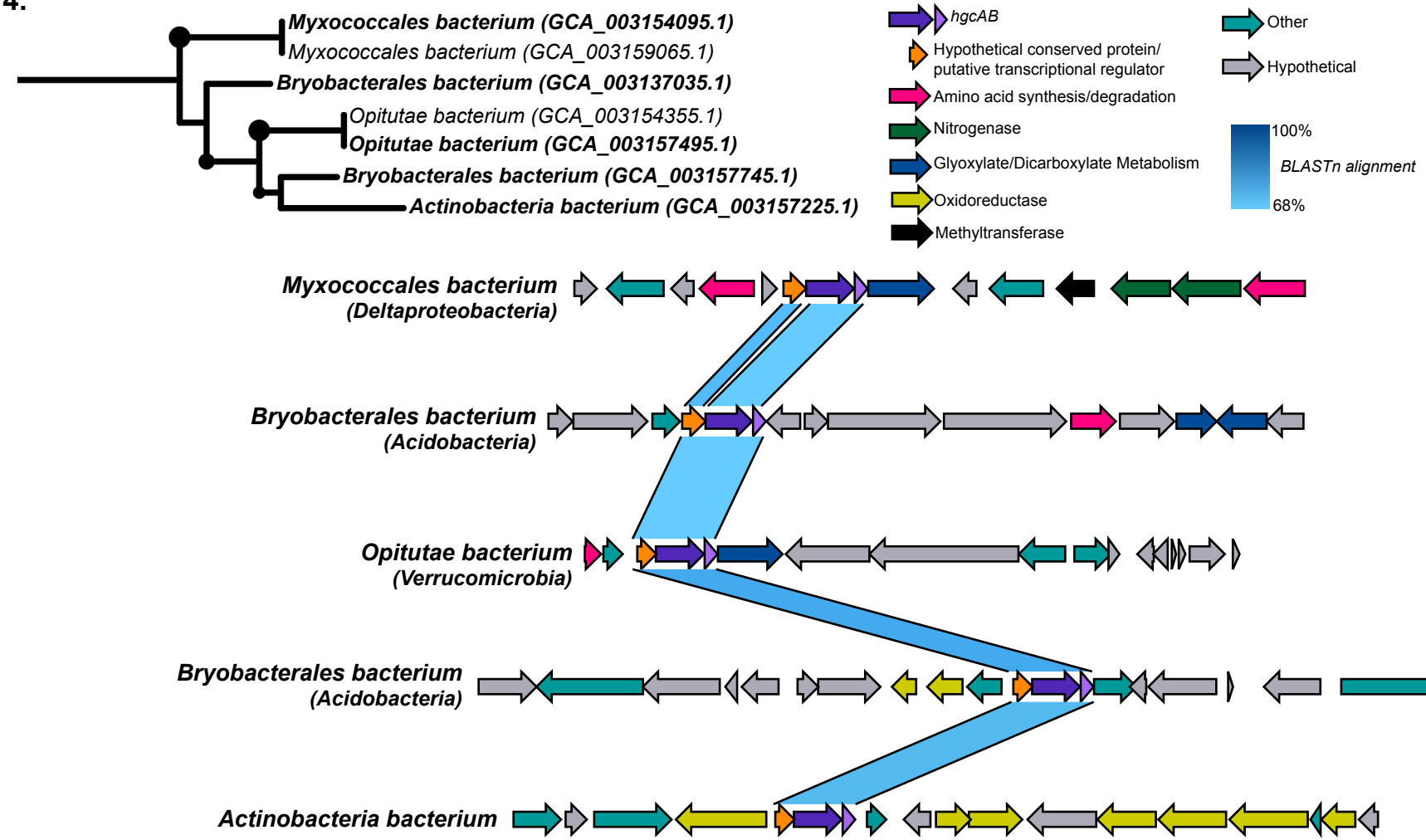
Myxococcales bacterium (GCA_003154095.1)
Myxococcales bacterium (GCA_003159065.1)
Bryobacterales bacterium (GCA_003137035.1)
Opitutae bacterium (GCA_003154355.1)
Opitutae bacterium (GCA_003157495.1)
Bryobacterales bacterium (GCA_003157745.1)
Actinobacteria bacterium (GCA_003157225.1)
hgcAB
Hypothetical conserved protein/ putative transcriptional regulator
Amino acid synthesis/degradation
Nitrogenase
Glyoxylate/Dicarboxylate Metabolism
Oxidoreductase
Methyltransferase
Other
Hypothetical
100%
BLASTn alignment
68%
Myxococcales bacterium (Deltaproteobacteria)
Bryobacterales bacterium (Acidobacteria)
Opitutae bacterium (Verrucomicrobia)
Bryobacterales bacterium (Acidobacteria)
Actinobacteria bacterium

5.

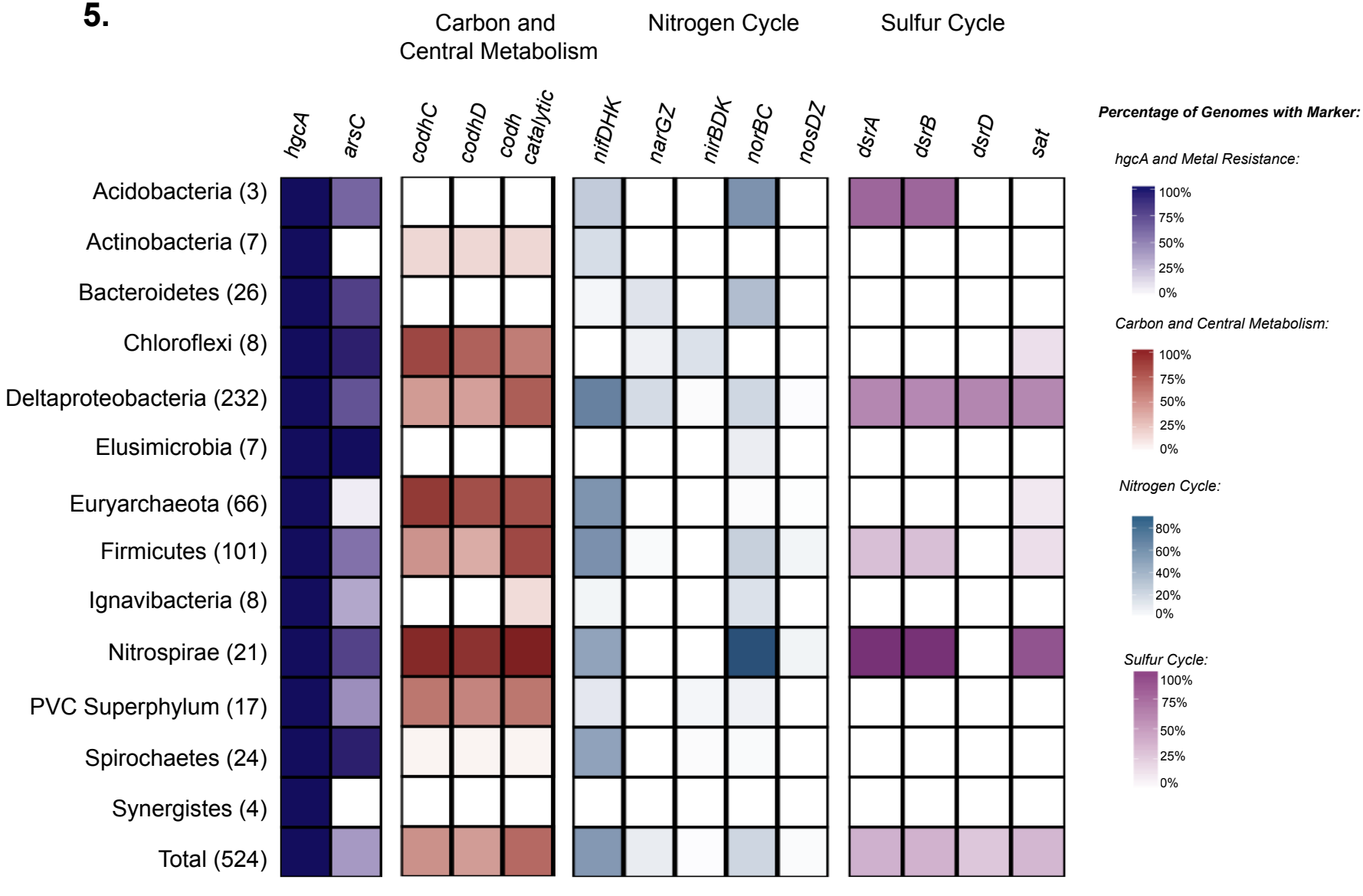
Carbon and Central Metabolism
Nitrogen Cycle
Sulfur Cycle
hgcA
arsC
codhC
codhD
codh catalytic
nifDHK
narGZ
nirBDK
norBC
nosDZ
dsrA
dsrB
dsrD
sat
Acidobacteria (3)
Actinobacteria (7)
Bacteroidetes (26)
Chloroflexi (8)
Deltaproteobacteria (232)
Elusimicrobia (7)
Euryarchaeota (66)
Firmicutes (101)
Ignavibacteria (8)
Nitrospirae (21)
PVC Superphylum (17)
Spirochaetes (24)
Synergistes (4)
Total (524)
Percentage of Genomes with Marker:
hgcA and Metal Resistance:
100%
75%
50%
25%
0%
Carbon and Central Metabolism:
100%
75%
50%
25%
0%
Nitrogen Cycle:
80%
60%
40%
20%
0%
Sulfur Cycle:
100%
75%
50%
25%
0%

6.

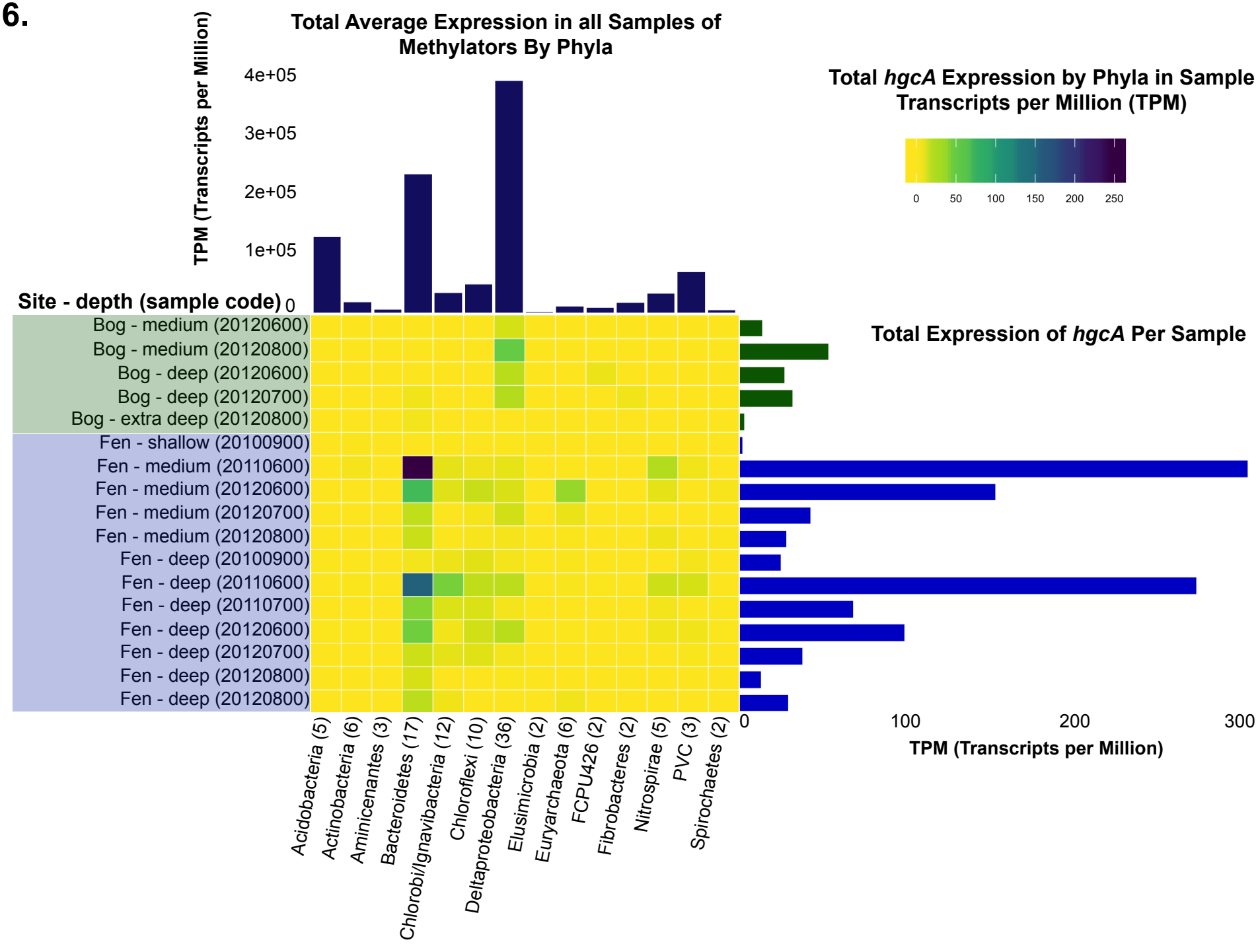
Total Average Expression in all Samples of Methylators By Phyla
TPM (Transcripts per Million)
4e+05
3e+05
2e+05
1e+05
0
Total hgcA Expression by Phyla in Sample Transcripts per Million (TPM)
0
50
100
150
200
250
Site - depth (sample code)
Bog - medium (20120600)
Bog - medium (20120800)
Bog - deep (20120600)
Bog - deep (20120700)
Bog - extra deep (20120800)
Fen - shallow (20100900)
Fen - medium (20110600)
Fen - medium (20120600)
Fen - medium (20120700)
Fen - medium (20120800)
Fen - deep (20100900)
Fen - deep (20110600)
Fen - deep (20110700)
Fen - deep (20120600)
Fen - deep (20120700)
Fen - deep (20120800)
Fen - deep (20120800)
Total Expression of hgcA Per Sample
0
100
200
300
TPM (Transcripts per Million)
Acidobacteria (5)
Actinobacteria (6)
Aminicenantes (3)
Bacteroidetes (17)
Chlorobi/Ignavibacteria (12)
Chloroflexi (10)
Deltaproteobacteria (36)
Elusimicrobia (2)
Euryarchaeota (6)
FCPU426 (2)
Fibrobacteres (2)
Nitrospirae (5)
PVC (3)
Spirochaetes (2)

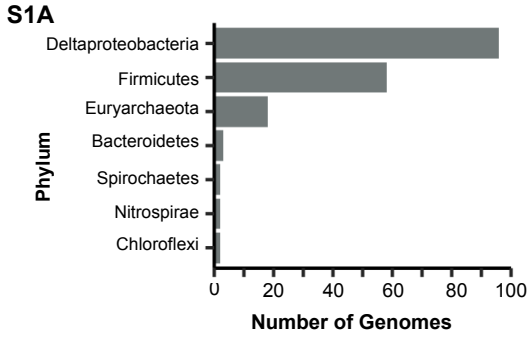
S1A
Deltaproteobacteria
Firmicutes
Euryarchaeota
Bacteroidetes
Spirochaetes
Nitrospirae
Chloroflexi
Phylum
0
20
40
60
80
100
Number of Genomes

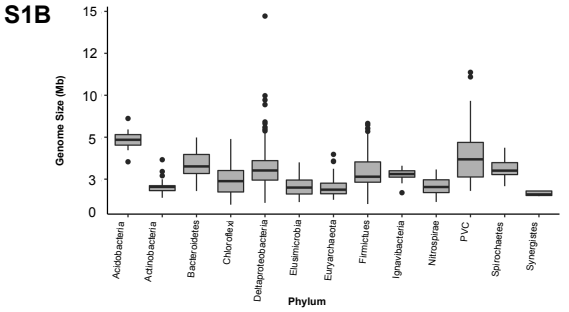
S1B
Genome Size (Mb)
0
3
5
10
12
15
Acidobacteria
Actinobacteria
Bacteroidetes
Chloroflexi
Deltaproteobacteria
Elusimicrobia
Euryarchaeota
Firmicutes
Ignavibacteria
Nitrospirae
PVC
Spirochaetes
Synergistes
Phylum

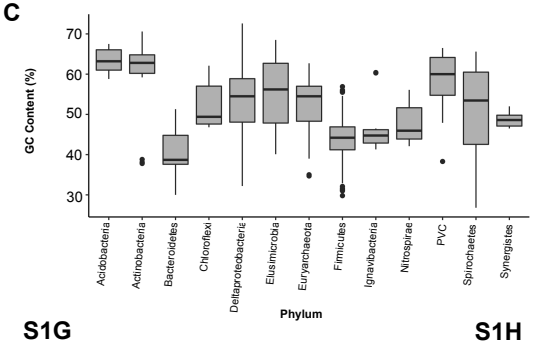
S1C
GC Content (%)
30
40
50
60
70
Acidobacteria
Actinobacteria
Bacteroidetes
Chloroflexi
Deltaproteobacteria
Elusimicrobia
Euryarchaeota
Firmicutes
Ignavibacteria
Nitrospirae
PVC
Spirochaetes
Synergistes
Phylum

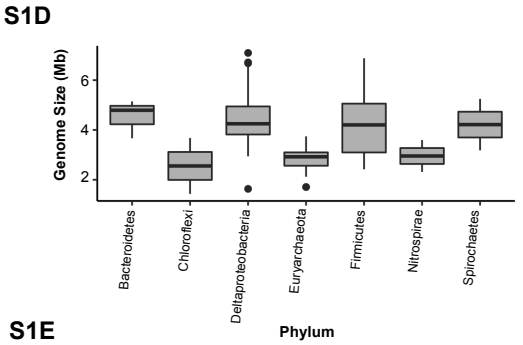
S1D
Genome Size (Mb)
2
4
6
Bacteroidetes
Chloroflexi
Deltaproteobacteria
Euryarchaeota
Firmicutes
Nitrospirae
Spirochaetes
Phylum

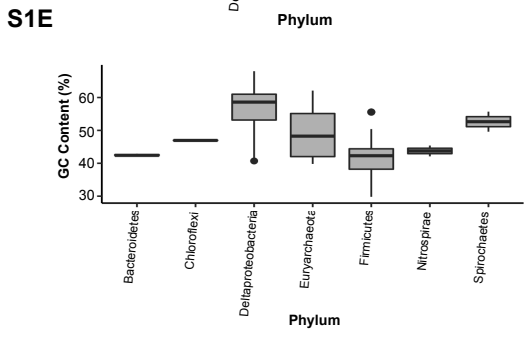
S1E
GC Content (%)
30
40
50
60
Bacteroidetes
Chloroflexi
Deltaproteobacteria
Euryarchaeota
Firmicutes
Nitrospirae
Spirochaetes
Phylum

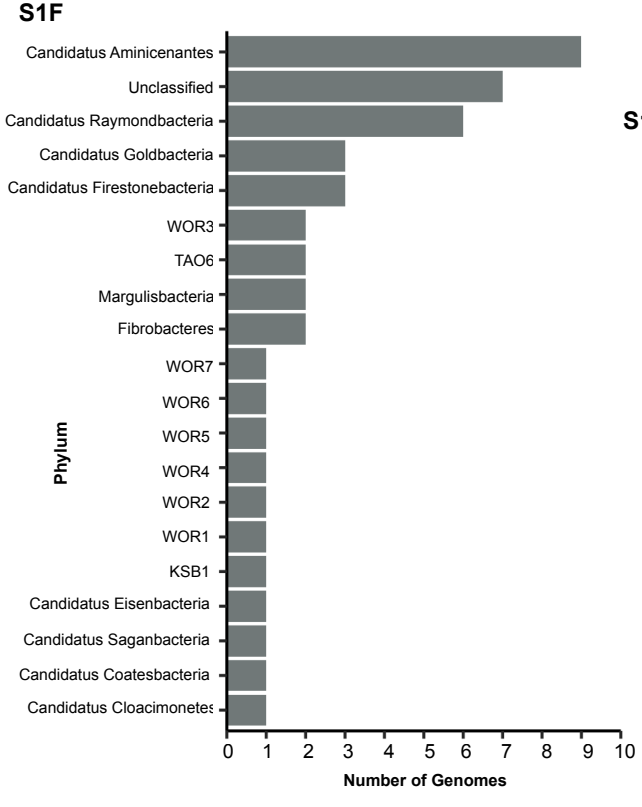
S1F
Candidatus Aminicenantes
Unclassified
Candidatus Raymondbacteria
Candidatus Goldbacteria
Candidatus Firestonebacteria
WOR3
TAO6
Margulisbacteria
Fibrobacteres
WOR7
WOR6
WOR5
WOR4
WOR2
WOR1
KSB1
Candidatus Eisenbacteria
Candidatus Saganbacteria
Candidatus Coatesbacteria
Candidatus Cloacimonetes
Phylum
0
1
2
3
4
5
6
7
8
9
10
Number of Genomes

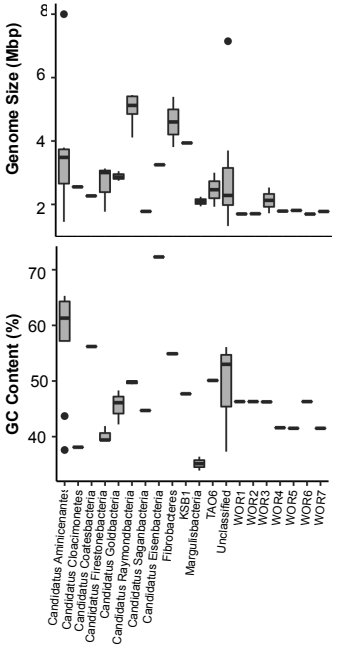
S1G
Genome Size (Mbp)
2
4
6
8
GC Content (%)
40
50
60
70
Candidatus Aminicenantes
Candidatus Cloacimonetes
Candidatus Coatesbacteria
Candidatus Firestonebacteria
Candidatus Goldbacteria
Candidatus Raymondbacteria
Candidatus Saganbacteria
Candidatus Eisenbacteria
Fibrobacteres
KSB1
Margulisbacteria
TAO6
Unclassified
WOR1
WOR2
WOR3
WOR4
WOR5
WOR6
WOR7

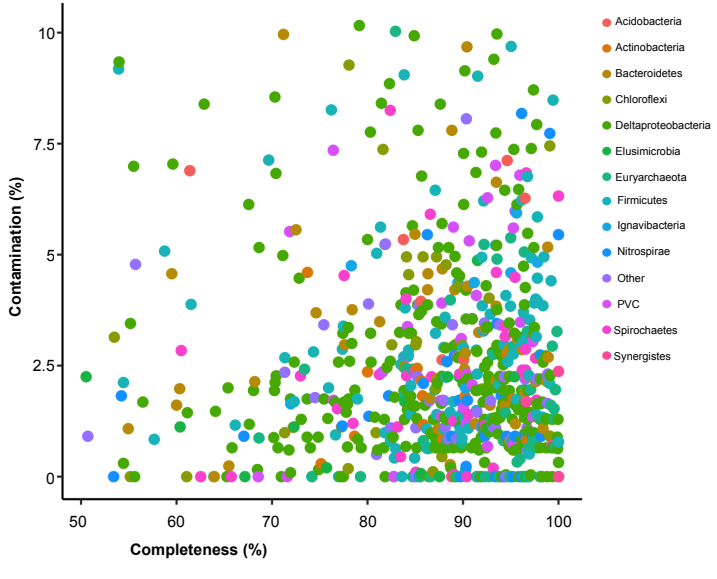
S1H
Contamination (%)
0
2.5
5
7.5
10
50
60
70
80
90
100
Completeness (%)
Acidobacteria
Actinobacteria
Bacteroidetes
Chloroflexi
Deltaproteobacteria
Elusimicrobia
Euryarchaeota
Firmicutes
Ignavibacteria
Nitrospirae
Other
PVC
Spirochaetes
Synergistes

S3.

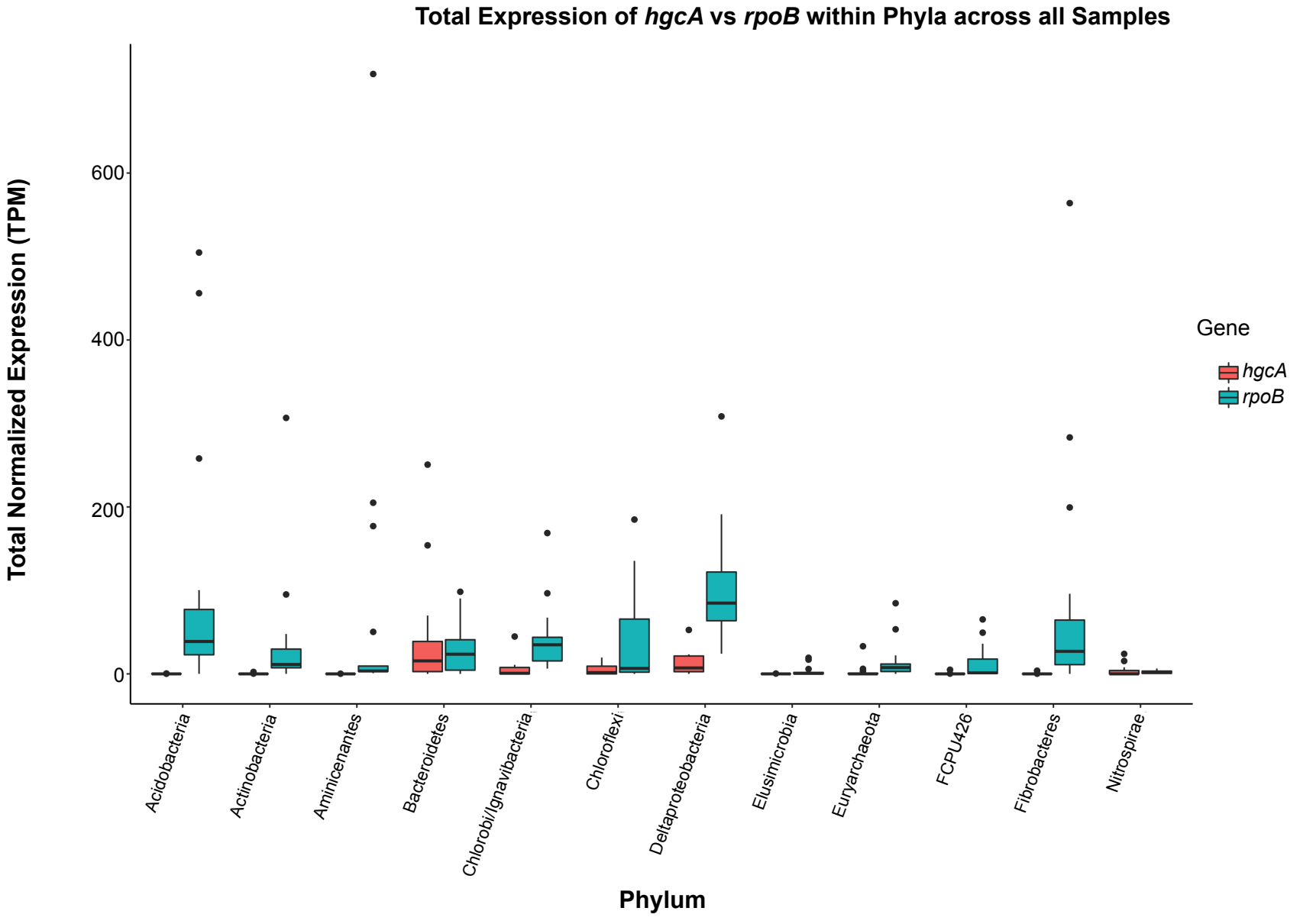
Total Expression of hgcA vs rpoB within Phyla across all Samples
Total Normalized Expression (TPM)
0
200
400
600
Gene
hgcA
rpoB
Acidobacteria
Actinobacteria
Aminicenantes
Bacteroidetes
Chlorobi/Ignavibacteria
Chloroflexi
Deltaproteobacteria
Elusimicrobia
Euryarchaeota
FCPU426
Fibrobacteres
Nitrospirae
Phylum